Relationship between anthropogenic CO_2 and the ^{13}C Suess effect in the North Atlantic Ocean

Arne Körtzinger[1] and Paul D. Quay
School of Oceanography, University of Washington, Seattle, Washington, USA

Rolf E. Sonnerup
Joint Institute for Study of the Atmosphere and Ocean, University of Washington, Seattle, Washington, USA

Received 20 April 2001; revised 12 March 2002; accepted 18 June 2002; published 4 January 2003.

[1] Temporal trends in oceanic dissolved inorganic carbon (DIC) and $\delta^{13}C$-DIC were reconstructed along five isopycnals in the upper 1000 m of the North Atlantic Ocean using a back-calculation approach. The mean anthropogenic DIC increase was 1.21 ± 0.07 μmol kg^{-1} yr^{-1} and the mean ^{13}C decrease was -0.026 ± 0.002‰ yr^{-1}, both in good agreement with the results from previous studies. The observed $\delta^{13}C$-DIC perturbation ratio is -0.024 ± 0.003‰ (μmol $kg^{-1})^{-1}$. Our results indicate that the North Atlantic is able to maintain equilibrium with the anthropogenic perturbation for DIC and follows it with decadal time lag for $\delta^{13}C$. A CFC-calibrated one-dimensional isopycnal advection-diffusion model is used to evaluate temporal DIC and $\delta^{13}C$ trends and perturbation ratios of the reconstructions. We investigate the time history of the air-sea CO_2 and ^{13}C disequilibria in the North Atlantic and discuss the importance of physical and biological processes in maintaining them. We find evidence that the North Atlantic Ocean is characterized by enhanced uptake of anthropogenic CO_2. Also, we use the model to examine how the time rate of change of $\delta^{13}C$ depends on changes in the temporal evolution of $\delta^{13}C$ in the atmosphere. The model evolution explains the curious result that the time rate of change of surface water $\delta^{13}C$ in the North Atlantic Ocean can exceed that observed concurrently in the atmosphere. Finally we introduce a powerful way of estimating the global air-sea pCO_2 disequilibrium based on the oceanic $\delta^{13}C$-DIC perturbation ratio. *INDEX TERMS:* 0312 Atmospheric Composition and Structure: Air/sea constituent fluxes (3339, 4504); 1803 Hydrology: Anthropogenic effects; 4806 Oceanography: Biological and Chemical: Carbon cycling; 4842 Oceanography: Biological and Chemical: Modeling; *KEYWORDS:* carbon cycle, anthropogenic carbon dioxide, ^{13}C Suess effect, advection-diffusion model, North Atlantic Ocean

Citation: Körtzinger, A., P. D. Quay, and R. E. Sonnerup, Relationship between anthropogenic CO_2 and the ^{13}C Suess effect in the North Atlantic Ocean, *Global Biogeochem. Cycles*, *17*(1), 1005, doi:10.1029/2001GB001427, 2003.

1. Introduction

[2] Human activities, such as burning of fossil fuels and land use changes, have emitted (and will continue to emit) anthropogenic CO_2 that is strongly depleted in the carbon isotope ^{13}C due to the preferential uptake of the light carbon isotope ^{12}C during the photosynthetic carbon fixation by plants. The resulting dilution of the atmospheric $^{13}C/^{12}C$ ratio by anthropogenic CO_2 emissions is known as the "^{13}C Suess effect" in analogy to (anthropogenic and natural) removal effects for the radioactive carbon isotope ^{14}C in atmospheric CO_2 first described by *Suess* [1953]. The oceanic ^{13}C Suess effect, i.e., the decrease of the $\delta^{13}C$ of dissolved inorganic carbon (DIC) as a consequence of CO_2 exchange with the atmosphere, provides a means of quantifying the oceanic uptake rate of anthropogenic CO_2 [*Quay et al.*, 1992; *Heimann and Maier-Reimer*, 1996; *Bacastow et al.*, 1996].

[3] Direct observation of anthropogenic changes in DIC and $\delta^{13}C$-DIC is hampered by a huge natural background (DIC) as well as significant seasonal and interannual variability and thus has only been feasible at two time series stations [e.g., *Bates et al.*, 1996; *Bacastow et al.*, 1996; *Winn et al.*, 1998; *Gruber et al.*, 1999; *Bates*, 2001]. Quantification of the oceanic Suess effect has proven to be particularly difficult due to the scarcity of quality historical $\delta^{13}C$ data. However, several promising methods have been proposed that exploit the information contained in oceanic ^{13}C measurements to quantify the ocean's uptake rate of CO_2 [*Quay et al.*, 1992; *Tans et al.*, 1993; *Bacastow et al.*, 1996; *Heimann and Maier-Reimer*, 1996; *Gruber and Keeling*, 2001]. In most of these the determination of the oceanic ^{13}C Suess effect is critical. This importance has

[1]Now at Department of Marine Biogeochemistry, Institute of Marine Research at the University of Kiel, Germany.

0886-6236/03/2001GB001427

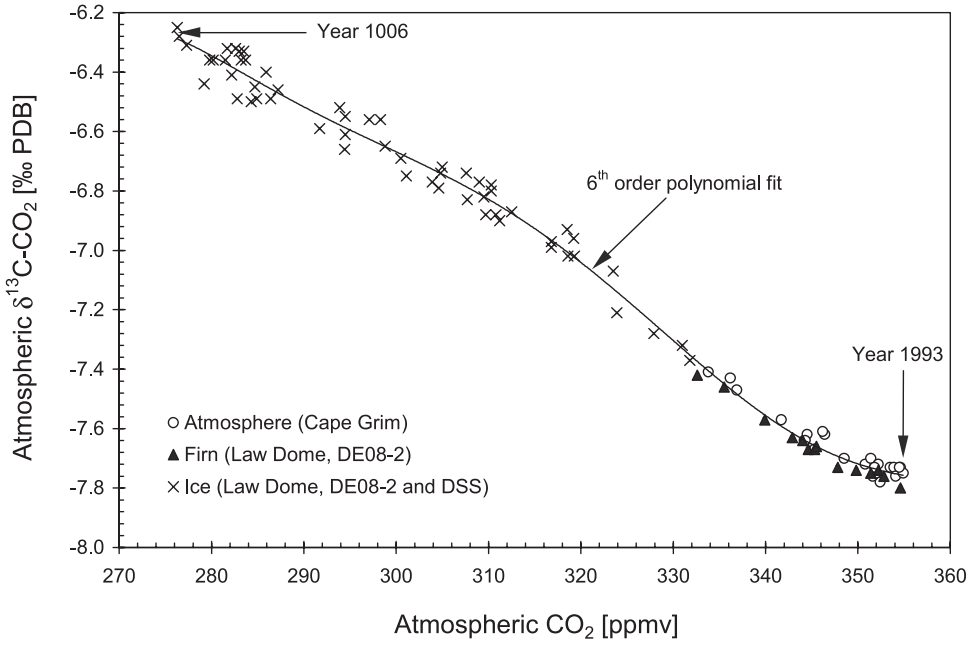

Figure 1. Plot of $\delta^{13}C$-CO_2 versus CO_2 measured on air samples taken at Cape Grim, Australia, or extracted from firn and ice samples of the Law Dome ice cores DE08-2 and DSS. A sixth order polynomial was fitted to the data representing the period 1006–1993. Data are from the studies of *Keeling and Whorf* [2000], *Neftel et al.* [1994], and *Francey et al.* [1999].

stimulated development of a method to determine the oceanic ^{13}C Suess effect from present-day data only using a back-calculation technique to reveal preformed $\delta^{13}C$-DIC values, whose temporal changes are estimated from water mass ages based on concurrent CFC measurements [*Sonnerup et al.*, 1999b].

[4] As pointed out by *Heimann and Maier-Reimer* [1996] the strong similarity of the atmospheric perturbation histories of CO_2 and ^{13}C (Figure 1) implies that the penetration of both oceanic perturbations must be similar. The relationship between changes in DIC and $\delta^{13}C$-DIC in the ocean should therefore reflect the atmospheric perturbation history of these tracers convoluted by the relative equilibration rates of these two tracers. *Keir et al.* [1998] have pointed out that the global relationship between oceanic DIC and $\delta^{13}C$-DIC changes provides a constraint on CO_2 exchange times between the atmosphere and the terrestrial biosphere. Unfortunately, knowledge of the relation between oceanic $\delta^{13}C$ and DIC changes is inadequate. Because the equilibration times of DIC and $\delta^{13}C$ between surface ocean and atmosphere differ by one order of magnitude, variability in surface water residence time with respect to gas exchange and circulation results in spatial variability of the oceanic $\delta^{13}C$-DIC perturbation ratio. While the global relationship may lie near 0.016‰ $(\mu mol\ kg^{-1})^{-1}$ [*Heimann and Maier-Reimer*, 1996], a recent study found that this ratio can vary substantially and could be as low as 0.007‰ $(\mu mol\ kg^{-1})^{-1}$ over much of the southern ocean [*McNeill et al.*, 2001].

[5] In this paper, we use the back-calculation approach of *Sonnerup et al.* [1999b] and extend it to DIC to estimate "preformed" $\delta^{13}C$-DIC and DIC values along five isopycnals in the North Atlantic Ocean. Using apparent CFC ages we reconstruct the temporal changes in these preformed properties. Next we explore the relationship between preformed DIC changes and preformed $\delta^{13}C$ changes in the North Atlantic Ocean. We use a simple, one-dimensional (1D) thermocline ventilation model to evaluate this relationship from a thermodynamic perspective and in the context of other published results. Finally we discuss the utility of our North Atlantic $\delta^{13}C$-DIC perturbation ratio in determining exchange times in the terrestrial biosphere and in quantifying ocean uptake of fossil-fuel CO_2.

2. Data

[6] Our analyses were carried out using the data acquired during the 1993 Ocean Atmosphere Carbon Exchange Study (OACES) cruise of R/V *Malcolm Baldrige* from 5°S to 65°N along 20°–29°W in the North Atlantic (4 July–30 August 1993). The data were retrieved from the NOAA Atlantic Oceanographic and Meteorological Laboratory (Miami, Florida, USA) public data server (http://www.aoml.noaa.gov/ocd/oaces/bottle_data.html).

[7] A systematic offset in the Winkler oxygen data was removed by adding 7.5 $\mu mol\ kg^{-1}$, as suggested in the data description file and by *Wanninkhof et al.* [1999]. Apparent oxygen utilization (AOU) was calculated as the difference between the oxygen solubility (calculated after *Weiss* [1970]) at the sample's temperature and salinity, and the sample's measured oxygen concentration. Although the measurement error of oxygen (after correction of the systematic offset) is only $\sim$1 $\mu mol\ kg^{-1}$, the error in AOU is dominated by the error in the assumption of oxygen saturation at the surface outcrop. *Gruber et al.* [1996] estimated an error of 4 μmol

kg^{-1} based on the observed deviation of wintertime surface oxygen concentrations from saturation.

[8] Dissolved inorganic carbon (DIC) was measured by coulometric titration following extraction of the CO_2 with an automated system known as SOMMA [*Johnson et al.*, 1993]. Total alkalinity (A_T) was determined by potentiometric titration with a system described in detail by *Millero et al.* [1993]. Based on regular measurements of certified reference material provided by Andrew Dickson from Scripps Institution of Oceanography (La Jolla, California, USA) the estimated accuracy of the carbon system parameters is 1.5 μmol kg^{-1} for DIC and 2.5 μmol kg^{-1} for A_T [*Millero et al.*, 1998; *Wanninkhof et al.*, 1999].

[9] The $\delta^{13}C$-DIC samples were poisoned with $HgCl_2$ immediately after collection. The CO_2 was extracted to 100 ± 0.5% using a helium stripping technique at the University of Washington, and the $^{13}C/^{12}C$ ratio of the extracted CO_2 was later measured on a Finnigan MAT 251 isotope ratio mass spectrometer. The overall precision of $\delta^{13}C$ analyses was ± 0.02‰ based on replicate analyses of standards and seawater samples [*Quay et al.*, 1992].

[10] Shipboard analyses of chlorofluorocarbons CFC-11 (CCl_3F) and CFC-12 (CCl_2F_2) were performed by a purge-and-trap extraction technique followed by gas chromatography with electron capture detection [*Bullister and Weiss*, 1988]. The precision of these analyses, based on measurements of replicate samples, is 0.01 pmol kg^{-1} or 1%, whichever is greater. Apparent CFC ages were obtained by converting measured CFC concentrations to equivalent air concentrations using known solubility relationships [*Warner and Weiss*, 1985]. These concentrations are compared with the atmospheric concentration history [*Walker et al.*, 2000] to obtain an apparent CFC age [*Doney and Bullister*, 1992].

[11] Water column data from all stations along the transect were interpolated linearly onto isopycnal surfaces from samples collected above and below. A history of annual mean atmospheric CO_2 concentrations was constructed from the Mauna Loa record of *Keeling and Whorf* [2000], covering the period from 1959 to the present, and the Siple Station ice core data of *Neftel et al.* [1994] for the period 1744–1953. The 1000-year high precision record of *Francey et al.* [1999] provided the history of atmospheric $\delta^{13}C$-CO_2. A sixth order polynomial fit function for the CO_2 versus $\delta^{13}C$-CO_2 relationship (Figure 1) described by *Francey et al.* [1999] was used to compute a history of annual mean $\delta^{13}C$-CO_2 from the combined Mauna Loa/Siple Station CO_2 record.

[12] Climatological data for temperature, salinity, wind speed, and mixed layer depth were used to estimate the outcrop latitude of each modeled isopycnal, and to force the advection-diffusion model. Sea surface temperature [*Levitus and Boyer*, 1994] and salinity [*Levitus et al.*, 1994] were taken from the Word Ocean Atlas 1994 (monthly 1° by 1° averages) and used to compute the wintertime maximum density along the meridional section. The location, where a wintertime density matching the isopycnal density was found, was taken as the outcrop location of that isopycnal. At each isopycnal's outcrop location representative data for sea surface temperature and sea surface salinity were taken from the World Ocean Atlas 1994 climatology data. Representative wind speed data (monthly 2° by 2° averages) were retrieved from the Comprehensive Ocean-Atmosphere Data Set (COADS) Release 1 Data Set. Finally, mixed layer depths, calculated with a fixed density criterion ($\Delta\sigma = 0.125$ kg m^{-3}), were taken from the World Ocean Atlas 1994 additional data [*Monterey and Levitus*, 1997].

3. Reconstruction of DIC^0 and $\delta^{13}C^0$ Along Isopycnals

3.1. Calculation Procedures

[13] The calculation of preformed DIC (DIC^0) and $\delta^{13}C$-DIC ($\delta^{13}C^0$) values, i.e., values which formed during the last contact with the atmosphere, requires quantification of biologically mediated changes in these quantities after removal from atmospheric contact. Biologically mediated changes in DIC are due to remineralization of organic matter and dissolution of biogenic carbonates at depth. A sample's AOU can be converted into the concurrent DIC increase using the stoichiometric $C_{org}/-O_2$ ratio of respiration, also referred to as "Redfield" ratio [*Redfield*, 1934; *Redfield et al.*, 1963]. By definition, the DIC change due to carbonate dissolution is half the resulting change in total alkalinity [*Pilson*, 1998]. The latter can be estimated from the difference between the observed sample alkalinity (A_T^{meas}) and the preformed alkalinity (A_T^0) in the water mass' outcropping area. A minor correction has to be applied to take account of the proton flux associated with the respiration of organic matter, which can be regarded as an in situ titration of total alkalinity. This correction is calculated from the Redfield $N/-O_2$ ratio of respiration and AOU. Hence, as originally suggested by *Brewer* [1978], DIC^0 can be calculated as follows:

$$DIC^0 = DIC - \left(\frac{C_{org}}{-O_2}\right)AOU - \frac{1}{2}\left[A_T^{meas} - A_T^0 + \left(\frac{N}{-O_2}\right)AOU\right] \quad (1)$$

[14] A number of studies have reestimated Redfield ratios of remineralization [e.g., *Takahashi et al.*, 1985; *Minster and Bouhladid*, 1987; *Anderson and Sarmiento*, 1994] but the $-O_2/C_{org}$ ratio has remained one of the least well determined ratios. This is because the presence of unknown amounts of anthropogenic CO_2 in the ocean effectively prohibited its reliable determination. In a recent study, *Körtzinger et al.* [2001a] applied the original techniques of *Takahashi et al.* [1985] and *Minster and Bouhladid* [1987] to DIC values that had been corrected for the anthropogenic CO_2 burden. The resulting $-O_2/C_{org}$ ratio of 1.34 ± 0.06 is in very good agreement with the average composition of phytoplankton [*Anderson*, 1995]. This value is slightly higher than the original value of 1.30 based on a stoichiometric model [*Redfield et al.*, 1963], and is within the error of the estimate (1.45 ± 0.15) of *Anderson and Sarmiento* [1994], which represents the mean of the original Redfield value and an $-O_2/C_{org}$ ratio of 1.60 measured on organic detritus [*Martin et al.*, 1987]. We used the value of 1.34 after *Körtzinger et al.* [2001a]. The $-O_2/N$ ratio is well constrained by various studies. Values range from 8.6 [*Redfield et al.*, 1963] to 10.6 [*Anderson and Sarmiento*,

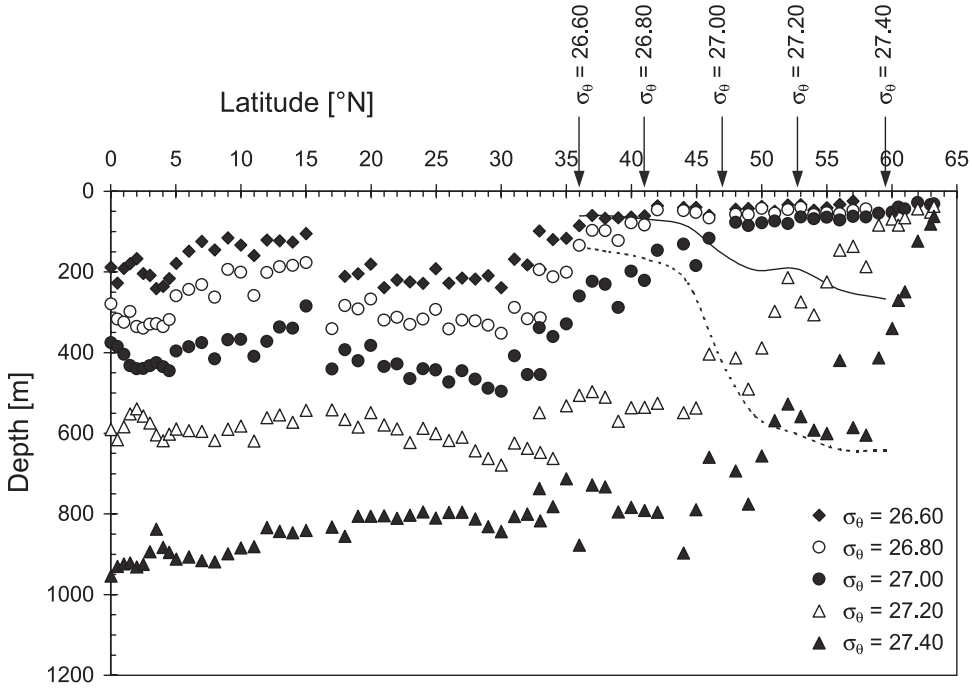

Figure 2. Depths of the five isopycnals σ_θ = 26.60 − 27.40 sampled along 20–29°W in the North Atlantic Ocean during 1993. The arrows indicate the estimated outcrop location of the isopycnals. Annual mean (black line) and winter maximum mixed layer depths (dashed line) are also shown.

1994]. We used a mean value of 9.6 which is in very good agreement with the results of *Takahashi et al.* [1985], *Minster and Bouhladid* [1987], and *Körtzinger et al.* [2001a]. Equation (1) can thus be rewritten as follows:

$$DIC^0 = DIC - 0.798AOU - 0.5\left(A_T^{meas} - A_T^0\right) \quad (2)$$

[15] The calculation of preformed DIC further requires estimation of a sample's preformed alkalinity (A_T^0). This is feasible on the basis of a multilinear regression on temperature and salinity. For details see Appendix A.

[16] Calculation of preformed $\delta^{13}C$-DIC ($\delta^{13}C^0$) is similar to that of DIC^0, except it requires estimates of the isotopic composition of the added organic matter and inorganic carbon [*Kroopnick*, 1985]

$$\delta^{13}C^0 = \frac{\left\{\delta^{13}C\,DIC - \delta^{13}C_{org}\left(\frac{C_{org}}{-O_2}\right)AOU - \frac{1}{2}\left[A_T^{meas} - A_T^0 + \left(\frac{N}{-O_2}\right)AOU\right]\delta^{13}C_{CaCO_3}\right\}}{\left\{DIC - \left(\frac{C_{org}}{-O_2}\right)AOU - \frac{1}{2}\left[A_T^{meas} - A_T^0 + \left(\frac{N}{-O_2}\right)AOU\right]\right\}} \quad (3)$$

where $\delta^{13}C$ is the $\delta^{13}C$ of DIC, $\delta^{13}C_{org}$ is the $\delta^{13}C$ of organic matter produced during primary production, and $\delta^{13}C_{CaCO_3}$ is the $\delta^{13}C$ of biogenic carbonates. The latter is typically within ± 1‰ of $\delta^{13}C$ of surface seawater DIC [*Bonneau et al.*, 1980]. Hence, calcification and carbonate dissolution have very little effect on the $\delta^{13}C$ and, unlike for DIC^0, the alkalinity terms in equation (3) can be neglected [*Sonnerup et al.*, 1999b]

$$\delta^{13}C^0 = \frac{\left[\delta^{13}C\,DIC - \delta^{13}C_{org}\left(\frac{C_{org}}{-O_2}\right)AOU\right]}{\left[DIC - \left(\frac{C_{org}}{-O_2}\right)AOU\right]} \quad (4)$$

[17] Equation (4) thus only requires knowledge of the $\delta^{13}C$ of organic matter produced during primary production. As an approximation we used the $\delta^{13}C$ of particulate organic matter which is typically of the order of −20‰ in most of the world oceans. We calculated $\delta^{13}C_{org}$ values for two latitude belts covering the study area from the data compiled by *Goericke and Fry* [1994]: Equator-20°N: −19.8 ± 0.9‰; 20°–65°N: −21.1 ± 1.8‰.

3.2. Isopycnal DIC^0 and $\delta^{13}C^0$ Distributions

[18] We have chosen five isopycnals (σ_θ = 26.60, 26.80, 27.00, 27.20, and 27.40 kg m^{-3}) along the 20°–29°W meridional transect in the North Atlantic, which are found at depths between 90 and 950 m (Figure 2) and thus in a domain of the ocean which is dominated by wind-driven circulation. Estimated outcrop locations cover the latitude range 36°–59.5°N. Apparent CFC-11 ages in subsurface samples at the outcrop locations are 1–6 years (Figure 3) and increase southward to maximum values of 22–45 years at 5°–10°N. CFC concentrations reached values near the detection limits (0.005–0.01 pmol kg^{-1}) only at the southern edge on the deepest isopycnal σ_θ = 27.40. Given the significantly longer atmospheric history of the $CO_2/^{13}C$ perturbation, all waters encountered on these isopycnals during this cruise must contain some anthropogenic CO_2.

[19] Preformed DIC (DIC^0) and $\delta^{13}C$-DIC ($\delta^{13}C^0$) were calculated using equations (2) and (4). Regressions of DIC^0 and $\delta^{13}C^0$ versus the apparent CFC-11 age show fairly consistent trends on all isopycnals (Figure 4). The mean DIC^0 versus CFC-11 age trend of 1.21 ± 0.07 μmol kg^{-1} yr^{-1} (Table 1) corresponds reasonably well with direct observations of the DIC increase: 1.7 μmol kg^{-1} yr^{-1} at

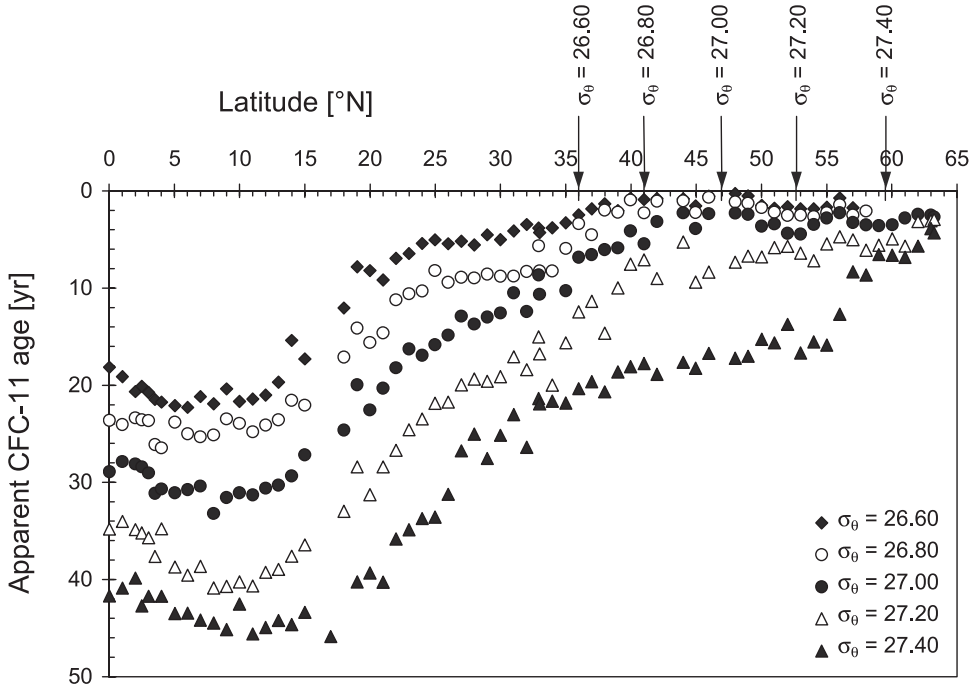

Figure 3. Apparent CFC-11 ages on five isopycnals along 20°–29°W in the North Atlantic Ocean during 1993. The arrows indicate the estimated outcrop location of the isopycnals.

the Bermuda Atlantic Time series Study (BATS) site [*Bates et al.*, 1996] and 0.72–1.37 μmol kg^{-1} yr^{-1} at the Hawaii Ocean Time series (HOT) site [*Winn et al.*, 1998]. It is slightly faster than the equilibrium DIC increase of 1.0 μmol kg^{-1} yr^{-1} calculated for a mean Revelle factor of 9.5 and a mean annual increase in atmospheric CO_2 concentrations of 1.5 ppmv yr^{-1} [*Keeling and Whorf*, 2000].

[20] The mean $\delta^{13}C^0$ versus CFC-11 age trend of −0.026 ± 0.002‰ yr^{-1} compares favorably with trends of −0.025 ± 0.002‰ yr^{-1} at Station "S" near Bermuda [*Bacastow et al.*, 1996; *Gruber et al.*, 1999] and −0.025 ± 0.002‰ yr^{-1} at station ALOHA (23°N, 158°W) in the North Pacific Ocean [*Gruber et al.*, 1999]. *Quay et al.* [1992] found a trend of −0.020‰ yr^{-1} (0.4‰ over the 20-year period 1970–1990) in the Pacific Ocean. The reconstruction of the method of *Sonnerup et al.* [1999b] on σ_θ = 27.2–27.4 in the North Atlantic was based on the same technique and data set but restricted to a smaller latitude band, only four data points, and gave slightly slower temporal changes of −0.018 ± 0.002‰ yr^{-1}. Our temporal $\delta^{13}C^0$ trend almost exactly matches the atmospheric Suess effect of −0.027 ± 0.001‰ yr^{-1} for the period 1962–1993 (calculated from the southern hemisphere $^{13}CO_2$ record of *Francey et al.* [1999]), and is indicative of a rather slow overturn of local surface waters in the North Atlantic Ocean [*Bacastow et al.*, 1996]. All of these estimates based on changes in $\delta^{13}C$-DIC are higher that the 0.018‰ yr^{-1} change found in a Sclerosponge further south near Jamaica (18°N, 77°W) during 1970–1990 [*Druffel and Benavides*, 1986; *Böhm et al.*, 1996].

[21] Generally, our temporal trends of DIC^0 and $\delta^{13}C^0$ fall on the high end of the range of published values. They should be regarded as upper limits because CFC-11 ages of >25 yr are biased young due to the non-linear trend in atmospheric CFC-11 prior to 1968 [*Doney and Bullister*, 1992; *Sonnerup*, 2001]. This effect is likely negligible on the shallow isopycnals σ_θ = 26.6 and 26.8, but on deep isopycnals may explain some of the discrepancy with the results of the study of *Sonnerup et al.* [1999b], which were restricted to ages of ≤17 years in the North Atlantic.

[22] Another potentially biasing effect is two-end-member mixing that occurs along the isopycnals. As no mixing correction was applied, any difference between northern and southern end-member values of preformed DIC and $\delta^{13}C$ lead to a bias in the inferred temporal changes of DIC^0 and $\delta^{13}C^0$. Clearly, the smaller the differences in the end-member preformed values, the smaller is the resulting bias. *Körtzinger et al.* [2001a] provide end-member values for potential temperature θ and DIC of three isopycnals (σ_θ = 27.0–27.2) in the Atlantic Ocean which can be used to assess the size of the mixing error. The fractions of the northern (f_N) and southern end-member (f_S) present at the southern edge of our data domain can be calculated from the end-members' preformed temperatures (θ^0_N and θ^0_S) and the potential temperature θ at the southern edge

$$f_N = (\theta - \theta^0_S)/(\theta^0_N - \theta^0_S) \quad (5)$$

[23] Based on these calculations, on isopycnals σ_θ = 27.0 and 27.2 about 40% of southern end-member water has been admixed at the southern edge around 5°–10°N. As the differences in present-day DIC^0 between the northern and southern end-member are about 11 μmol kg^{-1}, the mixing-related DIC change along the sampled part of the isopycnals is 4–5 μmol kg^{-1} at most. Based on this comparison of present-day DIC end-members, the resulting bias in the

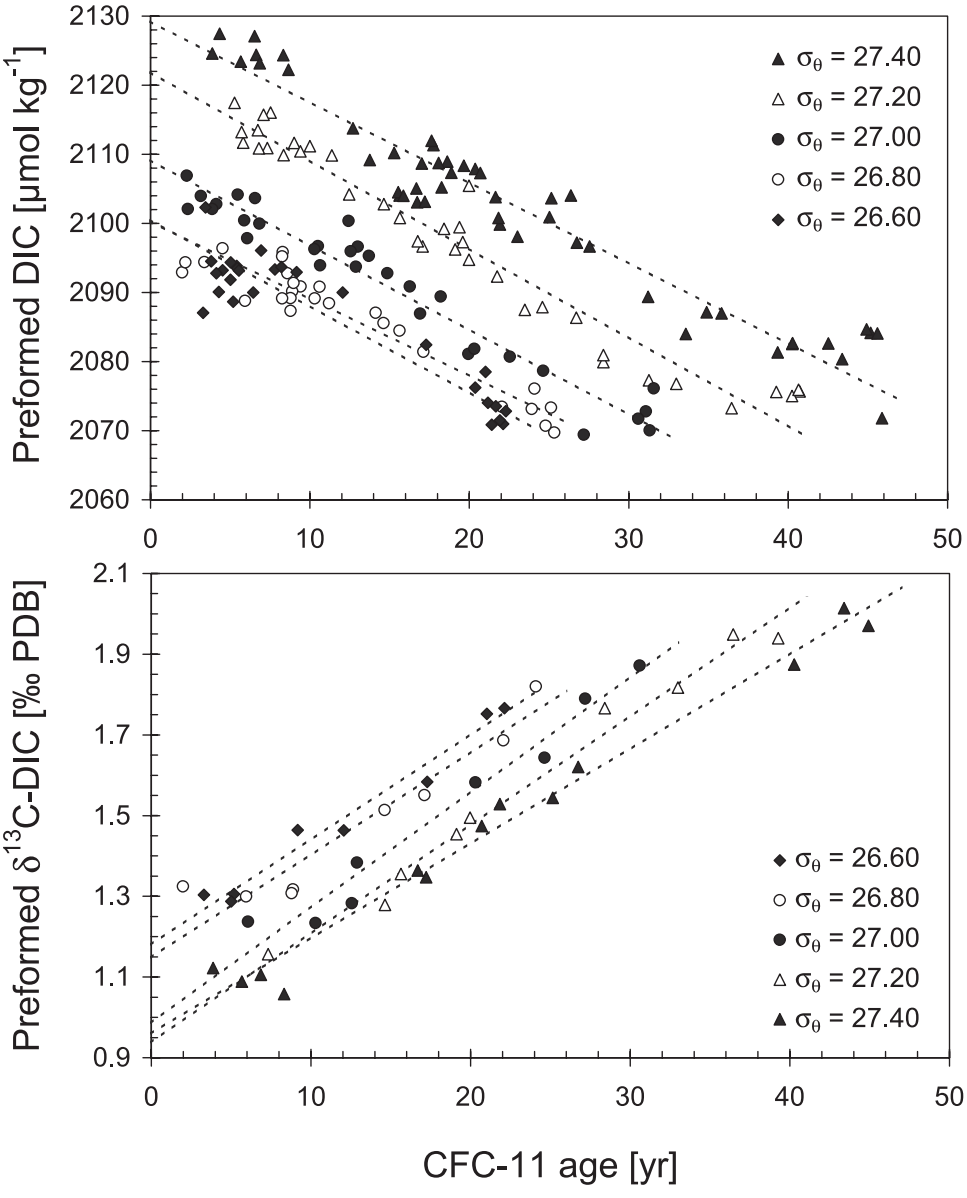

Figure 4. Plot of preformed DIC (top) and preformed δ^{13}C-DIC (bottom) versus apparent CFC-11 ages for five isopycnals along 20°–29°W in the North Atlantic Ocean. The dotted lines represent (model II) linear regressions of the data.

Table 1. The Temporal Change of DIC^0; and $\delta^{13}C^0$; Based on Apparent CFC-11 Ages for Five Isopycnals on a Meridional Section Along 20°–29°W in the North Atlantic Ocean

	Temporal DIC^0 Trend		Temporal $\delta^{13}C^0$ Trend	
Isopycnal	Data, µmol kg^{-1} yr^{-1}	Model, µmol kg^{-1} yr^{-1}	Data, ‰ yr^{-1}	Model, ‰ yr^{-1}
26.60	1.25 ± 0.09	0.91	−0.024 ± 0.002	−0.030
26.80	1.12 ± 0.07	0.94	−0.027 ± 0.003	−0.032
27.00	1.23 ± 0.06	0.97	−0.029 ± 0.002	−0.029
27.20	1.28 ± 0.05	1.01	−0.025 ± 0.001	−0.027
27.40	1.17 ± 0.05	0.98	−0.026 ± 0.001	−0.025
Mean	1.21 ± 0.07	0.96 ± 0.05	−0.026 ± 0.002	−0.029 ± 0.003

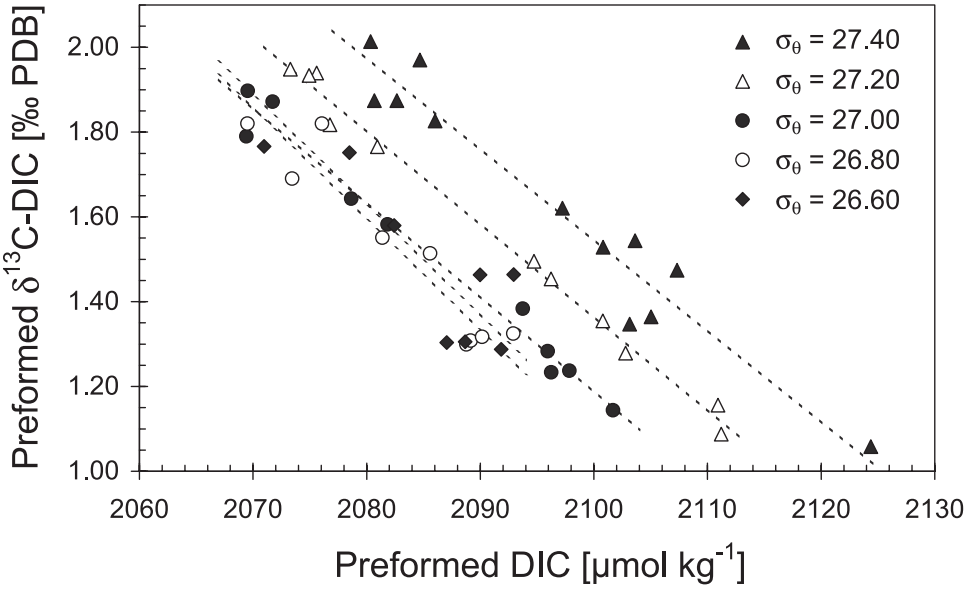

Figure 5. The relationship between preformed $\delta^{13}C$-DIC and preformed DIC for five isopycnals along 20°–29°W in the Northeast Atlantic Ocean. The dotted lines represent (model II) linear regressions to the data.

observed temporal tends of DIC^0 is <10%. As this bias tends to decrease the temporal trend, it partially offsets the bias toward faster changes favored by underestimation of water mass ages. Wintertime surface $\delta^{13}C$-DIC values are in the same range (1.7–2.2‰, Figure 2 in *Gruber et al.* [1999]) in the isopycnals' outcrop areas in the northern (36°–60°N) and southern (40°–50°S) hemispheres. Hence mixing likely has an even smaller effect on temporal $\delta^{13}C^0$ trends. In summary, although we cannot rule mixing biases out, we conclude that they are small and may be compensated by the previously discussed errors in apparent CFC ages.

[24] The "preformed-preformed" relationship between $\delta^{13}C^0$ and DIC^0 is fairly consistent on all isopycnals with a mean value of -0.024 ± 0.003‰ $(\mu mol\ kg^{-1})^{-1}$ (Figure 5 and Table 2). This implies larger relative $\delta^{13}C$ decreases than the model results of *Heimann and Maier-Reimer* [1996] using the three-dimensional Hamburg model of the oceanic carbon cycle HAMOCC 3. Their global ocean model results split into two trends of −0.016 and −0.019‰ $(\mu mol\ kg^{-1})^{-1}$ (calculated from their Figure 6), which may reflect some regional variability. *Keir et al.* [1998] found a slope of −0.016‰ $(\mu mol\ kg^{-1})^{-1}$ for a group of stations in the Northeast Atlantic Ocean based on anthropogenic CO_2 [*Körtzinger et al.*, 1998] and their reconstruction of anthropogenic $\delta^{13}C$ changes based on phosphate. Combination of temporal trends of DIC and $\delta^{13}C$ at stations BATS and HOT/ALOHA (see above) yields perturbation ratios of −0.015‰ $(\mu mol\ kg^{-1})^{-1}$ and −0.024‰ $(\mu mol\ kg^{-1})^{-1}$, respectively. These numbers, however, have a large uncertainty mainly due to the errors of the DIC trends. In the Southern Ocean, the $\delta^{13}C^0$ to DIC^0 change ratio was much smaller, ranging from 0.015 ± 0.005‰ $(\mu mol\ kg^{-1})^{-1}$ at 42°S down to 0.007 ± 0.005‰ $(\mu mol\ kg^{-1})^{-1}$ at 54°S [*McNeill et al.*, 2001].

[25] The theoretical relationship between $\delta^{13}C$ and DIC in an ocean fully equilibrating with the CO_2 and ^{13}C perturbations is shown in Figure 6. The tracer relationship shows two distinct slopes of -0.024 ± 0.001 and -0.032 ± 0.001‰ $(\mu mol\ kg^{-1})^{-1}$ during 1006–1968 and 1971–1993, respectively. This change in the slope between the atmospheric perturbations around 1970 (Figure 1) can already be seen in the record of *Francey et al.* [1999] who do not offer an explanation for it. However, this

Table 2. The "Preformed-Preformed" Relationship Between $\delta^{13}C^0$ and DIC^0 for Five Isopycnals on a Meridional Section Along 20°–29°W in the North Atlantic Ocean

		$\delta^{13}C^0$ versus DIC^0			
			Model, ‰ $(\mu mol\ kg^{-1})^{-1}$		
Isopycnal	CFC age range, yr	Data, ‰ $(\mu mol\ kg^{-1})^{-1}$	Overall	Pre-1970	Post-1970
26.60	3–22	−0.026 ± 0.006	−0.030	−0.030	−0.032
26.80	2–25	−0.026 ± 0.004	−0.031	−0.031	−0.032
27.00	3–32	−0.022 ± 0.001	−0.030	−0.027	−0.032
27.20	6–41	−0.022 ± 0.001	−0.029	−0.025	−0.032
27.40	5–46	−0.022 ± 0.002	−0.028	−0.025	−0.032
Mean		−0.024 ± 0.003	−0.030	−0.028	−0.032

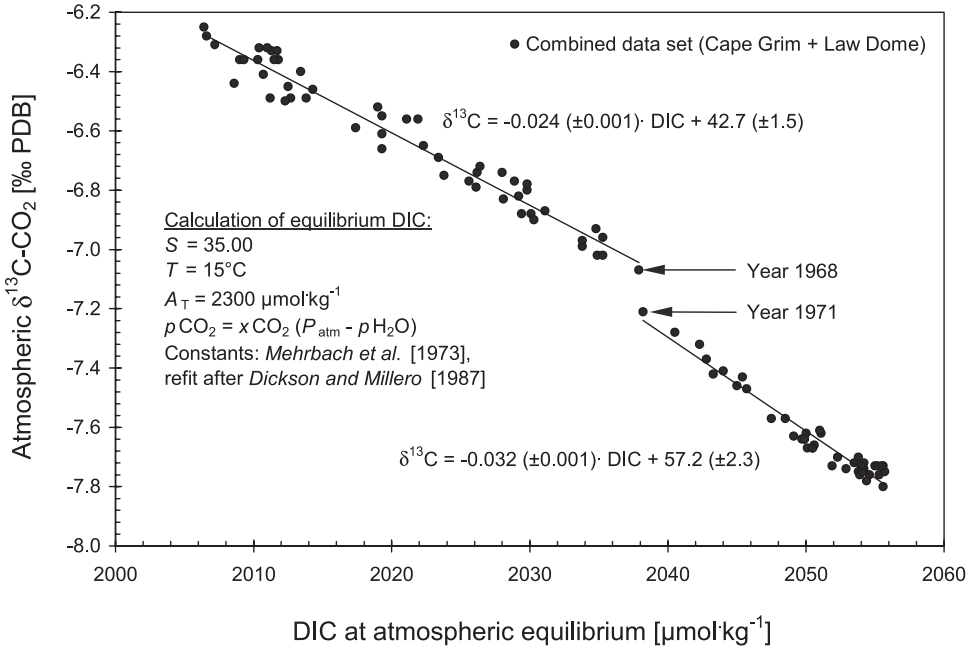

Figure 6. Relationship between atmospheric $\delta^{13}C$-CO_2 and the surface ocean DIC in equilibrium with the atmospheric CO_2 concentrations shown in Figure 1. The DIC increase at equilibrium with the changing atmosphere was calculated using the dissociation constants of carbonic acid described by *Mehrbach et al.* [1973] (refitted by *Dickson and Millero* [1987]) at $S = 35$, $T = 15°C$, and $A_T = 2300$ μmol kg^{-1}. These water properties yield a Revelle factor [*Sundquist et al.*, 1979] which is representative of the marine CO_2 system in the outcrop area of our five isopycnals. We also used pCO_2 at 100% humidity, which relates to the CO_2 mole fraction, xCO_2 (in ppmv), of the atmospheric CO_2 record of *Francey et al.* [1999] as follows: $pCO_2 = xCO_2(P_{atm} - pH_2O^{sat})$. Here P_{atm} is the total barometric pressure and pH_2O^{sat} is the water vapor saturation partial pressure, calculated using the method of *Weiss and Price* [1980].

slope change exactly coincides with the time when – based on the results of several models [*McGuire et al.*, 2001] – the terrestrial biosphere changed dramatically from more or less neutral to a net CO_2 sink. It can be speculated that the change in the atmospheric tracer relationship (and in the ocean) reflects the change in the net terrestrial CO_2 flux.

[26] The different perturbation relationships for the two time periods are reflected in our isopycnal reconstructions which range in apparent water mass ages between 22 years on shallow isopycnals ($\sigma_\theta = 26.60$) and >45 years on deeper isopycnals ($\sigma_\theta = 27.40$) and exhibit steeper slopes on younger isopycnals ($\sigma_\theta = 26.60$ and 26.80). Our results show $\delta^{13}C^0$ versus DIC^0 slopes which are steeper than those found by *Heimann and Maier-Reimer* [1996] and *Keir et al.* [1998] and closer to a scenario where the surface ocean DIC and $\delta^{13}C$ changes are in equilibrium with the atmosphere. Such a situation is likely not typical for the global ocean, and the North Atlantic may thus represent an upper extreme in the observed perturbation ratio. The inferred slow overturning in the North Atlantic can only be explained by the thermohaline circulation which leads to a net northward near surface transport of waters which remains in contact with the atmosphere for a considerable period of time, obviously long enough to permit full equilibration with both tracer signals. We study the reason for this finding using a numerical advection-diffusion model in section 4. We will also discuss the implications of these results in more detail in section 6.

4. Modeling of DIC^0 and $\delta^{13}C^0$ Along Isopycnals

4.1. Advection-Diffusion Model

[27] We use an advective-diffusive scheme to describe the meridional evolution of chemical tracers such as CFC-11 and CFC-12, and to reconstruct anthropogenic changes of DIC and the $^{13}C/^{12}C$ ratio of DIC along selected isopycnal horizons in the Atlantic Ocean

$$\frac{dC}{dt} = -v\frac{dC}{dx} + K\frac{d^2C}{dx^2} \tag{6}$$

Here C represents the tracer concentration, v is the equatorward meridional component of the along-isopycnal advection velocity, K is the along-isopycnal eddy diffusivity, t is time, and x is the meridional distance.

[28] The model uses a 1° latitudinal spacing and is marched forward in time using a 1-month time step. The temporal change of tracer concentrations is calculated using centered in time, centered in space (CTCS, or "leapfrog") differencing of the advection terms and the DuFort-Frankel scheme for the diffusion terms [*Fletcher*, 1988; *Sonnerup et al.*, 1999a]. Here we run the model beginning in 1934 and 1765 for CFCs and anthropogenic

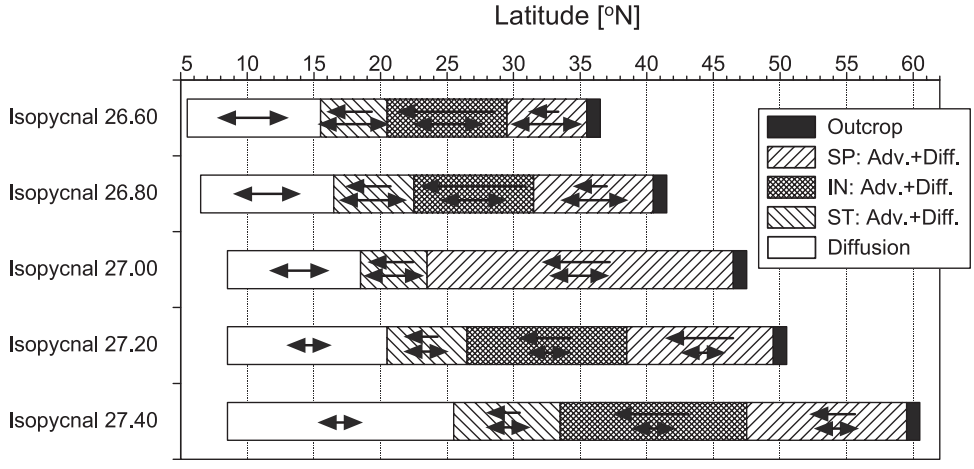

Figure 7. Schematic diagram of the location of southern boundaries, outcrop regions, and advection regions as defined in the advection-diffusion model (SP = subpolar, IN = intermediate, ST = subtropical). The arrows (not to scale) indicate the relative magnitude of along-isopycnal meridional velocities and horizontal diffusivities. The location of the model boundaries corresponds to inflections in the main features seen in the meridional CFC-11 distribution during 1993.

CO_2/^{13}C, respectively. The model's transport parameters, v and K, are varied to fit the CFC-11 and CFC-12 distribution in 1993, as measured during the OACES cruise, to the North Atlantic Ocean (20°W). The CFC-calibrated model is then used to predict the distribution of anthropogenic DIC and $\delta^{13}C$ changes.

[29] The boundary condition applied at the outcrop box assumes that the surface seawater remains at the degree of equilibrium with atmospheric CFC-11 and CFC-12 observed on these isopycnals at the outcrop location during the 1993 cruise. We assumed an outcropping period of 3 months for CFCs and used winter month averages (JFM) of climatological T and S. The calibration of the model's transport parameters is sensitive to the along-isopycnal slope of the CFC profile rather than absolute CFC concentrations. The model calibration is nearly insensitive to the length of the outcropping period. Using a 12 month per year outcropping period, with annual means of T and S, yielded virtually identical velocities and diffusivities as the 3 months per year outcrop and required only 5–10% higher saturation levels. We apply a zero diffusive flux boundary condition for CFC, DIC, and $\delta^{13}C$-DIC at the southern boundary, where no meridional gradients in these properties were observed (Figures 3 and 9).

[30] For all isopycnals, CFC saturation was within 8% of equilibrium with the 1993 atmosphere (92–107%). Transport within the subtropical gyre is dominated by advection, and CFC gradients largely reflect the near-linear increase in atmospheric CFC concentrations during the 1970s and 1980s. Advection velocity is thus determined by the slope of the CFC gradient. Based on the shape of the CFC-11 distribution on each isopycnal, several regimes – here identified as "subpolar", "intermediate", and "subtropical" – can be identified and were assigned individual velocities. Figure 7 schematically depicts the different regions as defined for each isopycnal. Values of model parameters are summarized in Table 3.

[31] South of the tropical-subtropical front (16°–26°N), which represents the front between North (NACW) and South Atlantic Central Water (SACW) [*Klein and Tomczak*,

Table 3. Model Parameters (Advection Velocity, Eddy Diffusivity, CFC Saturation at the Outcrop) Used in the Advection-Diffusion Model[a]

Isopycnal	Southward Velocity[b], cm s^{-1}			Horizontal Diffusivity, m^2 s^{-1}	CFC Saturation, %	DIC_0 Pre-Ind., μmol kg^{-1}	A_T^0, μmol kg^{-1}	Revelle Factor Mean[c]	$f_{CO_3^{2-}}$ Mean[c]
	SP	IN	ST						
26.60	0.13	1.80	0.25	1900	93	2031	2382	9.5	0.111
26.80	0.16	1.65	0.25	1800	92	2035	2362	9.9	0.103
27.00	0.53		0.25	1000	100	2045	2347	10.3	0.094
27.20	0.60	0.33	0.20	700	107	2057	2335	10.8	0.086
27.40	0.24	0.76	0.20	700	99	2071	2327	11.4	0.079

[a]DIC^0 was calculated from preformed alkalinity (derived from T and S) by assuming equilibrium with the pre-industrial atmosphere. The carbon system parameters reflect the characteristics of the marine CO_2 system at the outcrop location.

[b]Abbreviations "SP", "IN", and "ST" refer to the "subpolar", "intermediate" and "subtropic" model regions, respectively (see Figure 7).

[c]As the ocean takes up anthropogenic CO_2, some of its buffer capacity is consumed. As a consequence, the Revelle factor increases at equilibrium by about 10% and the carbonate fraction decreases by around 21% (1765–1993). In the model we used the means between pre-anthropogenic and 1993 Revelle factors.

1994], the flow is predominantly zonal and we assumed that meridional transport here is due solely to along-isopycnal eddy diffusion. As a result, diffusivities are slightly sensitive to the location of the southern boundary which was placed in the center of the no-CFC-gradient regime and moved northward from 6°N to 9°N on successively deeper isopycnals. Diffusivities were adjusted to yield the best fit to the data south of the tropical-subtropical front and decrease with increasing depth from 1900 to 700 $m^2\ s^{-1}$ (Table 3). These numbers compare well with literature values from 1800 $m^2\ s^{-1}$ [*Jenkins*, 1991] to 500 $m^2\ s^{-1}$ [*Armi and Stommel*, 1983]. Individual isopycnal diffusivities were assumed to be constant over the full meridional extent of the model.

[32] Our simple 1D-advection-diffusion model does not include the possibility of diapycnal mixing, which might account for part of the discrepancy between model results and reconstruction. However, *Speer* [1997] demonstrated that diapycnal mixing is weak (indistinguishable from zero) in the thermocline (σ_θ = 26.6–27.6) of the North Atlantic Ocean. Furthermore the area investigated is not influenced by boundaries, passages etc. that might give rise to strong cross-isopycnal mixing. *Sonnerup et al.* [1999a] found that diapycnal CFC fluxes accounted for <15% of CFC ventilation into the subtropical Pacific thermocline. On the other hand, *Klein and Tomczak* [1994] found evidence for unidirectional diapycnal mixing in the front between NACW and SACW (near 15°N on our section), which they attributed to double diffusion. This process, however, is likely to affect only shallower isopycnals ($\sigma_\theta \leq 27.00$) in the frontal region.

[33] The importance of zonal transports, which cannot be represented by our meridional advection-diffusion model, has to be assessed. We compared our meridional transect with CFC, DIC, and $\delta^{13}C$ data (where available) from several zonal transects intersecting at 51°N (R/V *Meteor* cruises 39/2 + 4 in 1997 [*Körtzinger et al.*, 1999]), at 48°N (R/V *Meteor* cruises 30/2 in 1994 [*Körtzinger et al.*, 1998] and 39/3 in 1997), and at 24.5°N (OACES 24N North Atlantic Cruise in 1998, http://www.aoml.noaa.gov/ocd/oaces/24n98.html). In the upper 1000 m of the eastern North Atlantic basin these sections show very little zonal variability of all three tracers (CFC, DIC, and $\delta^{13}C$). Significant gradient are evident not only near the European/African shelf and above the mid-Atlantic ridge but also at deeper levels. Based on these findings we estimate that biases due to zonal transports are likely small overall.

4.2. Model Simulation of Anthropogenic CFC, $^{13}CO_2$, and $^{13}CO_2$ Perturbations

4.2.1. Calculation Procedures

[34] Our CFC-calibrated advection-diffusion model is used to describe the along-isopycnal penetration of the perturbation signals of CO_2 and ^{13}C into the North Atlantic Ocean. Atmospheric histories of CO_2 and $^{13}CO_2$ are prescribed at the outcrop where the resulting air-sea net flux of CO_2 and $^{13}CO_2$ is calculated. The model is initialized with CO_2 and ^{13}C in equilibrium with the pre-industrial atmosphere (as outlined in Appendix B). Processes that kept the real pre-industrial surface ocean CO_2 system at a certain degree of air-sea disequilibrium (e.g., biology, mixing) are not reflected in the model and affect the predicted DIC and $\delta^{13}C$-DIC values as discussed below. For anthropogenic DIC and $\delta^{13}C$-DIC it was found that an outcropping period of 12 months was required in order for the model ocean to take up realistic amounts of CO_2. Therefore we used annual climatological means of *T*, *S*, mixed layer depth, and wind speed in the model runs for DIC and $\delta^{13}C$.

[35] The net flux of CO_2, F_{12}, across the air-sea interface can be described by a bulk formula

$$F_{12} = k\ K_H\left(pCO_2^g - pCO_2^{sea}\right) \tag{7}$$

where k is the transfer (or piston) velocity, K_H is the solubility of CO_2 in seawater, and pCO_2^g and pCO_2^{sea} are the partial pressures of CO_2 in seawater and air, respectively. In order to simplify calculations, we used the mole fraction of CO_2 in dry air (xCO_2) instead of the partial pressure (pCO_2). These two quantities are linked by the total barometric pressure and the water vapor saturation partial pressure (see caption of Figure 6). If no surface skin temperature effect is present, P_{atm} and pH_2O^{sat} are identical for pCO_2^g and pCO_2^{sea} and the use of xCO_2 instead of pCO_2 represents only a very small error in F_{12}, ranging from −0.5% to +2% over the temperature range 4–26°C (at P = 1 atm). The solubility of CO_2, K_H, was calculated following the study of *Weiss* [1974]. For the wind speed dependence of the transfer velocity k, we used the quadratic parameterization for climatological winds of *Wanninkhof* [1992]. It should be noted that this bulk formula is strictly only valid for total CO_2, i.e., the sum of $^{12}CO_2$ and $^{13}CO_2$. We assume this equation also to be valid for $^{12}CO_2$ as this represents about 98.9% of the CO_2.

[36] The net flux of $^{13}CO_2$, F_{13}, across the air-sea interface can be described in a similar fashion

$$F_{13} = \alpha_k k \alpha_{aq-g} K_H \left(R^g_{CO_2} pCO_2^g - \frac{R_{DIC}}{\alpha_{DIC-g}} pCO_2^{sea} \right) \tag{8}$$

where α_k is the kinetic fractionation factor for $^{13}CO_2$ gas exchange, α_{aq-g} is the equilibrium fractionation factor for CO_2 gas dissolution, and α_{DIC-g} is the fractionation factor between seawater DIC and CO_2 in air. $R^g_{CO_2}$ and R_{DIC} represent the $^{13}C/^{12}C$ ratios of CO_2 in air and DIC, respectively. More details on the derivation of equation (8) and the parameterizations used for the fractionation factors are given in Appendix C.

[37] The fluxes of $^{12}CO_2$ and $^{13}CO_2$ are calculated according to equations (7) and (8) at every time step. These fluxes per unit area of the air-sea interface (μmol m^{-2} $month^{-1}$) are then converted into water column concentration changes of DIC and $DI^{13}C$ (both in μmol kg^{-1}) by using the annual mean mixed layer depth (mld) and density (ρ). As the model advects and diffuses the tracer DIC, the air-sea exchange itself depends on the concentration difference of CO_2 across the air-sea interface (equation (7)), so a conversion has to be made back and forth between DIC and pCO_2. This was done using the Revelle (or homogeneous buffer) factor f_R, which represents the quotient of the relative increases in pCO_2 and DIC at equilibrium and

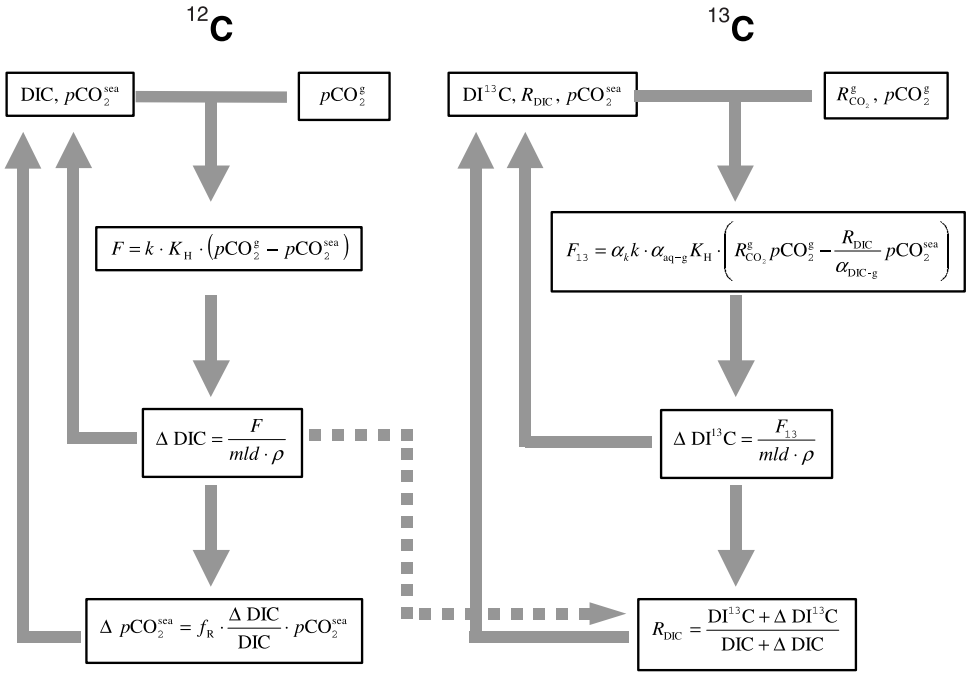

Figure 8. The steps involved in the calculation of the air-sea flux of $^{12}CO_2$ and $^{13}CO_2$ at the outcrop and the concurrent change in the tracers DIC and R_{DIC} during every time step of the advection-diffusion model.

constant temperature, salinity, and alkalinity [*Sundquist et al.*, 1979]

$$f_R = \left[\left(\frac{\partial pCO_2}{pCO_2} \right) \Big/ \left(\frac{\partial DIC}{DIC} \right) \right]_{T,S,A_T} \quad (9)$$

From this, the pCO_2^{sea} change was calculated

$$\Delta pCO_2^{sea} = f_R \frac{\Delta DIC}{DIC} pCO_2^{sea} \quad (10)$$

[38] Similarly, the change in the $DI^{13}C$ inventory (= $R_{DIC}DIC$) is calculated from F_{13}, and the resulting change in R_{DIC} is derived from $\Delta DI^{13}C$ and ΔDIC. The complete calculation procedure for DIC and R_{DIC} is shown in Figure 8.

[39] The Revelle factor is not a constant. As the ocean takes up anthropogenic CO_2, the Revelle factor increases and the ocean's CO_2 uptake capacity decreases. The total increase of the Revelle factor since pre-industrial times is on the order of 10%. We use the mean of the factors for 1765 and 1993, calculated assuming equilibrium with the atmosphere. The simplification of using a constant mean rather than a variable Revelle factor has very little consequence on the results. The difference in modeled 1993 meridional DIC gradient between a constant and a variable Revelle factor is 0.1–0.5 μmol kg^{-1} across the whole section.

4.2.2. Model Results for DIC^0 and $\delta^{13}C^0$

[40] The CFC-calibrated advection-diffusion model was used to predict DIC and R_{DIC} changes from pre-industrial equilibrium as a consequence of the prescribed measured atmospheric perturbation. As the model does not include biologically mediated CO_2 changes, the model parameters DIC and R_{DIC} are directly comparable to the properties DIC^0 and $\delta^{13}C^0$ (expressed as R^0_{DIC}) reconstructed from field data. This assumes, of course, that values chosen for $-O_2/C_{org}$, $-O_2/N$, A^0_T, and $\delta^{13}C_{org}$ in equations (2) and (4) represent actual conditions in the Northeast Atlantic Ocean, and that wintertime oxygen saturation levels are indeed close to 100% for all the isopycnal outcrops.

[41] Magnitude and shape of the temporal change of DIC^0 and $\delta^{13}C^0$ as well as the $\delta^{13}C^0$-DIC^0 relationship are generally in very good agreement with the reconstruction (Figure 9 and Tables 1 and 2). The modeled temporal change of DIC^0 of 0.96 ± 0.05 μmol kg^{-1} yr^{-1} is about 20% smaller than the reconstructed change (Figure 4 and Table 1) but in close agreement with the equilibrium increase of 1.0 μmol kg^{-1} yr^{-1} for a Revelle factor of 9.5. The modeled $\delta^{13}C^0$ temporal change of −0.029 ± 0.003‰ yr^{-1}, however, agrees well with both the reconstruction (Figure 4 and Table 1) and the atmospheric trend (−0.027 ± 0.001‰ yr^{-1}).

[42] The model $\delta^{13}C^0$-DIC^0 relationship has a slope of −0.030 ± 0.003‰ (μmol $kg^{-1})^{-1}$ which is 25% steeper than the reconstructed slope (Table 2). This difference is due primarily to the difference between reconstructed and modeled temporal DIC^0 changes. A closer look at the model results reveals that the two different equilibrium trends for the pre-1970 and post-1970 periods (Figure 6) are mirrored in the model output (Table 2). The change in the mean $\delta^{13}C^0$-DIC^0 slopes is determined by the range in water mass ages found on a particular isopycnal, i.e., by the degree to which the two different periods are represented on that isopycnal.

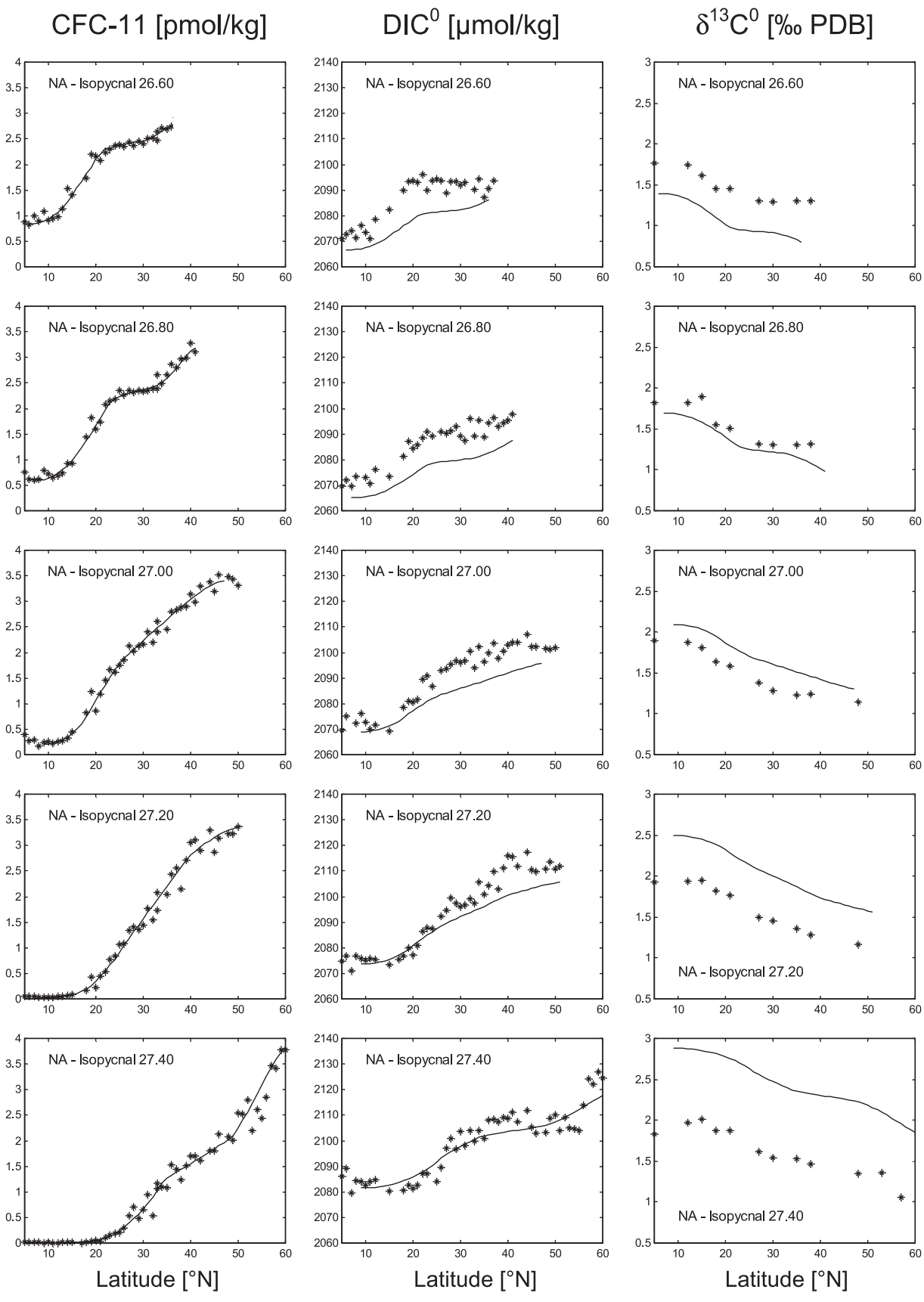
CFC-11 [pmol/kg]
DIC⁰ [µmol/kg]
δ¹³C⁰ [‰ PDB]
NA - Isopycnal 26.60
NA - Isopycnal 26.80
NA - Isopycnal 27.00
NA - Isopycnal 27.20
NA - Isopycnal 27.40
Latitude [°N]
Latitude [°N]
Latitude [°N]

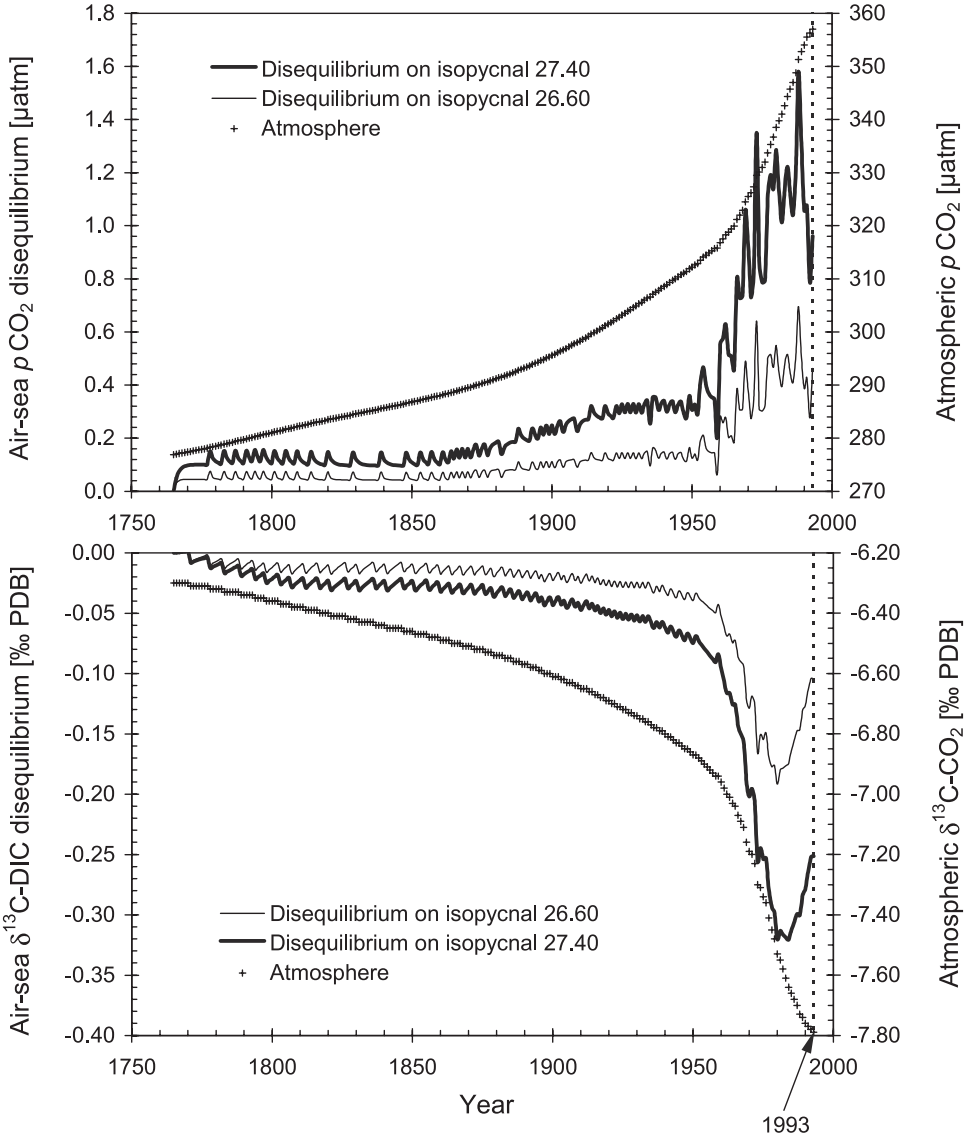

Figure 10. Temporal evolution of the air-sea disequilibrium of pCO_2 (top) and $\delta^{13}C$-DIC (bottom) in the advection-diffusion model. Only the deepest (σ_θ = 27.40) and shallowest isopycnal (σ_θ = 26.60) are shown. Also shown is the time history of atmospheric CO_2 (top) and $\delta^{13}C$-CO_2 (bottom).

[43] The model surface seawater pCO_2 at the outcrop closely follows the atmospheric pCO_2 (Figure 10). The developing small air-sea pCO_2 disequilibrium in the model reaches maximum values between 0.6 µatm (σ_θ = 26.60) and 1.5 µatm (σ_θ = 27.40) during the last 30 years. This is on the order of the annual increase of atmospheric pCO_2 (1.5 µatm) and reflects the 1-year equilibration timescale of CO_2. In contrast, the model outcrop $\delta^{13}C$ does not keep pace with the atmospheric perturbation. Although initialized at equilibrium, modeled $\delta^{13}C$ develops a significant air-sea disequilibrium (Figure 10) increasing with time toward maximum values between −0.19‰ (σ_θ = 26.60) and −0.32‰ (σ_θ = 27.40). Like for pCO_2, this disequilibrium is building up very slowly as the rate of change in atmospheric $\delta^{13}C$-CO_2 remains moderate. Around the middle of the 20th century the rate of change in $\delta^{13}C$-CO_2 increases significantly reaching maximum values during the 1970s. The maximum air-sea disequilibrium during the last decades is about ten times the annual atmospheric $\delta^{13}C$-CO_2 decrease (−0.027‰ yr^{-1}) beautifully reflecting the 10-year equilibrium timescale of ^{13}C.

[44] This variable air-sea disequilibrium for $\delta^{13}C$ explains the increase in the modeled temporal $\delta^{13}C^0$ trend from −0.025‰ yr^{-1} on isopycnal σ_θ = 27.40 to values below

Figure 9. (opposite) Comparison of data (symbols) and model results (lines) for CFC-11 concentration (left column), preformed DIC (DIC^0, center column), and preformed $\delta^{13}C$-DIC ($\delta^{13}C^0$, right column) for five isopycnals along 20°–29°W in the North Atlantic Ocean.

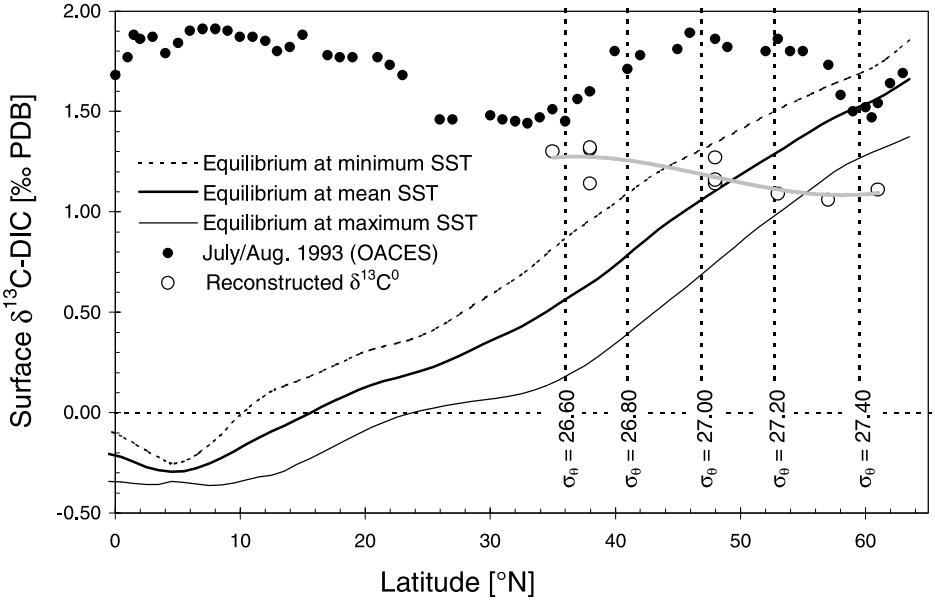

Figure 11. Comparison of 1993 equilibrium and measured surface δ^{13}C-DIC values as well as modeled preformed δ^{13}C-DIC ($\delta^{13}C^0$) along 20°–29°W in the North Atlantic Ocean. Equilibrium values are given at mean, maximum, and minimum climatological temperature under the 1993 atmosphere. The mean atmospheric δ^{13}C-CO_2 of −7.87‰ was calculated from 1993 flask samples taken at NOAA CMDL Cooperative Air Sampling Network stations Iceland (ICE, 52°N/20°W) and Barbados (RPB, 13°N/59.5°W); data taken from CMDL server (ftp://ftp.cmdl.noaa.gov/ccg/).

−0.030‰ yr^{-1} on the shallowest isopycnals (Table 1). While the latter comprise an age range of only 20 years, apparent water mass ages on isopycnal σ_θ = 27.40 span a range of more than 40 years (Figure 4). As the model ^{13}C air-sea disequilibrium shows a maximum in the early 1980s and decreases thereafter, it is possible for the oceanic Suess effect to be even greater than the atmospheric Suess effect for the last 10–15 years. During this period the oceanic $\delta^{13}C$ change not only follows (with roughly a 10-year time lag) the atmospheric Suess effect of −0.025 ± 0.001‰ yr^{-1} but partially compensates the higher disequilibrium that has built up during the 1970s. The shorter time window sampled on the shallowest isopycnals reflects this enhanced Suess effect more than does the longer time window of deeper isopycnals which reflects the opposite situation in the 1960s and 1970s, when the oceanic Suess did not keep pace with the atmospheric Suess effect and a growing air-sea disequilibrium was found (Figure 10).

5. Air-Sea Disequilibria

5.1. The Air-Sea Disequilibrium of CO_2

[45] There is disagreement over the absolute values of DIC^0 between model results and data. This is due to the fact that, unlike the model ocean, the real ocean in most places is not in equilibrium with the atmosphere nor has it been in pre-industrial times [*Sarmiento and Sundquist*, 1992]. Modeled and reconstructed DIC^0 values are in close agreement only on the deepest isopycnal σ_θ = 27.40 (Figure 9). Going up in the water column, modeled DIC^0 is increasingly lower than reconstructed DIC^0. On the shallowest isopycnal σ_θ = 26.60, a mean DIC^0 difference of around 11 μmol kg^{-1} (17°–26°N) is found which corresponds to a surface pCO_2 difference of about 22 μatm. The disequilibrium increases with decreasing age and is generally largest for waters having been ventilated most recently. The disagreement between modeled and reconstructed DIC^0 is always smallest or even nonexistent at the southern edge indicating that the surface ocean in the outcropping area was closer to equilibrium at the time these oldest waters were last ventilated. Hence, the reconstructed along-isopynal DIC^0 change is higher than what is expected from the atmospheric CO_2 increase alone which is in agreement with the results from BATS [*Bates et al.*, 1996; *Bates*, 2001].

[46] The more-than-expected increase in DIC could be explained by a combination of two factors – the nonlinearity of the marine CO_2 system and the strong undersaturation typically found in the North Atlantic Ocean. Our results as well as model results [e.g., *Meier-Reimer and Hasselmann*, 1987; *Sarmiento et al.*, 1992] indicate that the surface ocean is able to follow the atmospheric CO_2 perturbation. The corresponding increase in surface DIC, however, not only depends on the atmospheric CO_2 increase itself but also on the natural CO_2 disequilibrium maintained by other processes. For an ocean area remaining significantly undersaturated with respect to atmospheric CO_2 while following the secular CO_2 rise, the total DIC increase for a given atmospheric change is higher than for an ocean starting at equilibrium. Accordingly a naturally supersaturated ocean area will show a smaller anthropogenic DIC signal. Being initialized at equilibrium, our model cannot represent this effect, which should be contained though in the reconstructions.

[47] The North Atlantic Ocean (north of 30°–35°N) is significantly undersaturated with respect to atmospheric pCO_2 [*Takahashi et al.*, 1995, 1997, 2002]. This strong CO_2 sink results from the combined effects of biological carbon uptake and the cooling of water moving northward as part of the subtropical gyre circulation and of the thermohaline circulation. The North Atlantic Ocean should thus be one of the primary ocean regions to be characterized by an enhanced DIC increase. Obviously the opposite would be true for natural source regions such as the tropical oceans. Our North Atlantic Ocean results may therefore represent an upper extreme in the global context.

[48] An enhanced uptake of anthropogenic CO_2 could also be caused by possible climate feedback mechanisms [*Joos et al.*, 1999] which might already be at work in the real ocean. While this is entirely possible, it is hard to detect such feedbacks in the field. If acting as proposed, however, the feedback mechanisms should become more important and more readily detectable as climate change progresses.

5.2. The Air-Sea Disequilibrium of $\delta^{13}C$

[49] There is also disagreement between the absolute values of $\delta^{13}C^0$ of model results and the reconstruction, indicating that the surface ocean is not at air-sea equilibrium for ^{13}C. It is well established that there are several processes at work that keep the surface ocean from achieving isotopic equilibrium [*Broecker and Maier-Reimer*, 1992]. Four primary factors can be identified that can cause air-sea disequilibrium of ^{13}C: (1) export production of organic matter, (2) mixing/upwelling of subsurface water into the mixed layer, (3) net air-sea exchange of CO_2 [*Lynch-Stieglitz et al.*, 1995], and (4) the temperature dependence of the equilibrium fractionation between DIC and CO_2 in the air ($\alpha_{DIC\text{-}g}$).

[50] In the following we try to explain observed patterns of (measured and reconstructed) surface water $\delta^{13}C$-DIC in the North Atlantic Ocean. For this purpose, we looked at five data sets (Figure 11): $\delta^{13}C$ measured on surface samples (upper 20 m) taken during the OACES cruise in July/August, reconstructed $\delta^{13}C^0$ values from subsurface samples near the outcrop locations of the five isopycnals, and the equilibrium surface $\delta^{13}C$ at climatological mean, maximum, and minimum outcrop temperatures in equilibrium with the 1993 atmosphere.

[51] Measurements of surface $\delta^{13}C$ were made on samples taken during summertime (July/August 1993). In contrast, our reconstructed $\delta^{13}C^0$ values reflect wintertime ventilation conditions. In the absence of any seasonality in surface $\delta^{13}C$ values, these two data sets should coincide. This seems to be the case in the southern part of the section (south of approximately 30°N), which is essentially a permanently oligotrophic system that does not show significant wintertime surface nutrient concentrations nor a winter-to-summer drawdown of surface DIC [*Körtzinger et al.*, 2001b]. A similarly small seasonality in surface ocean $\delta^{13}C$ has been reported by *Gruber et al.* [1998] for the Bermuda time series station at 32°N (seasonal $\delta^{13}C$ cycle of 0.2–0.3‰).

[52] North of about 35°N, the elevation of summer $\delta^{13}C$ above wintertime $\delta^{13}C^0$ is primarily due to export production of organic matter, which has already fully depleted nitrate and phosphate south of 57°N at the time of the measurement (August 1993). In contrast, nitrate (2.0–5.9 μmol kg^{-1}) and phosphate (0.29–0.45 μmol kg^{-1}) were still available north of 57°N comprising roughly 25–50% of wintertime surface concentrations. Consequently, $\delta^{13}C$ values are less strongly elevated above wintertime preformed $\delta^{13}C^0$ values. Both measured $\delta^{13}C$ and reconstructed $\delta^{13}C^0$ seem to converge around 30–35°N, the transition region toward the permanently oligotrophic system further south [see also the work of *Körtzinger et al.*, 2001b].

Table 4. Values Employed in Mass Balance Calculation After Equation (11)

Parameter (unit)	Symbol	Value
Atmosphere		
Pre-industrial inventory at 278 ppmv (Pg C)	M_a^0	610[a]
Mean 1960–1993 inventory at 335.3 ppmv (Pg C)	M_a	738[a]
	ΔM_a	128
Pre-industrial atmospheric $\delta^{13}C$-CO_2 (‰)	δ_a^0	−6.3
Mean 1960–1993 atmospheric $\delta^{13}C$-CO_2 (‰)	δ_a	−7.3
	$\Delta\delta_a$	−1.0
Ocean		
Mean DIC within penetration depth (μmol kg^{-1})	CT	2000
Pre-industrial $\delta^{13}C$-DIC (‰)	δ_s^0	2.2[b]
Biosphere		
Change in $\delta^{13}C$ (‰)	$\Delta\delta_b$	−1[c]
Fossil Fuel Source		
Mean 1960–1993 fossil fuel $\delta^{13}C$-CO_2 (‰)	δ*	−27.9[d]

[a] 1 ppmv CO_2 = 2.2 Pg C.
[b] Calculated using the pre-industrial atmospheric $\delta^{13}C$-CO_2 and an ocean-wide average $\varepsilon_{DIC\text{-}g}$ of 8.59 (at area-weighted mean SST of 18.4°C).
[c] *Keir et al.* [1998].
[d] *Andres et al.* [2000], after their Figure 3.5.

[53] Measured surface $\delta^{13}C$-DIC values are in the range 1.4–1.9‰ everywhere along the transect representing isotopic air-sea equilibrium only around 60°N. Toward the south surface $\delta^{13}C$-DIC is increasingly enriched in ^{13}C by up to 2‰ above air-sea equilibrium. Reconstructed preformed $\delta^{13}C^0$ is near atmospheric equilibrium (at annual mean T) around 47°N (outcrop of isopycnal σ_θ = 27.00). The enrichment of preformed $\delta^{13}C^0$ above air-sea equilibrium south of 47°N can be attributed to two major factors: export production of organic carbon from the mixed layer and the temperature dependence of as documented in the equilibrium curves of Figure 11.

[54] The observed meridional trend in preformed $\delta^{13}C^0$ with lower (reconstructed) values in the north and higher (measured) values toward south, however, cannot be explained by export production alone. One possible candidate for maintaining this gradient could be air-sea exchange of CO_2. Annual net CO_2 fluxes following the study of *Takahashi et al.* [1995] are near zero (±1 × 10^{12} g C yr^{-1} for 4° (latitude) × 5° (longitude) area) south of 35°N but show significant net uptake north of here (3–7 × 10^{12} g C yr^{-1} for 4° × 5° area). Our simple model calculations, however, indicate that the net CO_2 flux is less depleted in ^{13}C at low temperatures. Furthermore the depletion in the net CO_2 flux increases with decreasing ΔpCO_2. Thus our tests indicate that net uptake of CO_2 in the North Atlantic is likely not a major contributor to the observed meridional $\delta^{13}C^0$ gradient.

[55] We also looked into the $\delta^{13}C$ signature of the upward DIC flux (calculated at each station from the $\delta^{13}C$-DIC slope

of samples in the upper 200 m). In the southern half of our section this upward DIC flux is characterized by $\delta^{13}C$ values of $-14 \pm 2‰$. In the northern part, however, the DIC is much more depleted with $\delta^{13}C$ values of $-22 \pm 1‰$. Such differences can be explained by the winter mixed layer depth, which does not exceed values of 40 m south of 20°N and increases moderately to about 200 m toward 45°N. Around 45°N a steep increase in maximum wintertime mixed layer depths is observed with maximum values of up to 700 m (Figure 2). This pronounced gradient in winter mixed layer depth has consequences on the characteristics of the surface ocean CO_2 system. In the area of shallow mixing, the DIC source from below the mixed layer does not mirror the isotopic signature of particle flux and is probably more strongly influenced by advection and lateral processes. Where winter mixed layers are deep, the carbon system may be more self-contained, i.e., most of the respiration of exported particles and thus most of the imprint of its ^{13}C signature occurs within a depth horizon that is reentrained into the mixed layer during wintertime. This indicates that the upward DIC flux may contribute significantly to the observed meridional gradient in preformed $\delta^{13}C^0$.

6. The $\delta^{13}C^0$ and DIC^0 Relationship

[56] The "preformed-preformed" relationship between $\delta^{13}C^0$ and DIC^0 is useful in several ways. First of all, the relationship provides a link between the change of the oceanic carbon inventory and the ^{13}C Suess effect. If representative of the world ocean, it can be used for direct conversion between global inventory changes of DIC and ^{13}C. This relationship thus provides a means of cross-checking independent inventory estimates and potentially a powerful constraint on model-based simulations.

[57] Second, *Keir et al.* [1998] demonstrated that the "preformed-preformed" relationship can be used to constrain the size of the exchangeable terrestrial biosphere, i.e., that part of the terrestrial biosphere (e.g., vegetation, wood, detritus) which actively exchanges with the atmosphere on the timescale of the atmospheric CO_2 perturbation. *Keir et al.* [1998] adapted the atmosphere, ocean, and terrestrial biosphere $^{12}CO_2$ and $^{13}CO_2$ budget of *Quay et al.* [1992] to examine the relationship between $\delta^{13}C^0$ ($\Delta\delta_s$) and DIC^0 (ΔC_T)

$$\frac{\Delta\delta_s}{\Delta C_T} = \frac{\delta^* - \delta_s^0}{C_T} + \frac{\left[\Delta M_a\left(\delta^* - \delta_s^0\right) - \left(M_a^0 + \Delta M_a\right)\Delta\delta_a - M_b^0\Delta\delta_b\right]}{\Delta M_s C_T} \quad (11)$$

where δ^* and δ_s^0 are the mean $\delta^{13}C$ values of fossil fuel source CO_2 and pre-industrial ocean DIC (here C_T), respectively. $\Delta\delta_a$ and $\Delta\delta_b$ are the changes since pre-industrial times in atmospheric $\delta^{13}C$-CO_2 values and terrestrial biosphere $\delta^{13}C$ values, respectively. M_a^0 and M_b^0 denote pre-industrial carbon inventories of the atmosphere and the terrestrial biosphere, respectively. ΔM_a is the change in the atmospheric carbon inventory while ΔM_s denotes the change of the oceanic carbon inventory. Actual values chosen for these parameters are shown in Table 4.

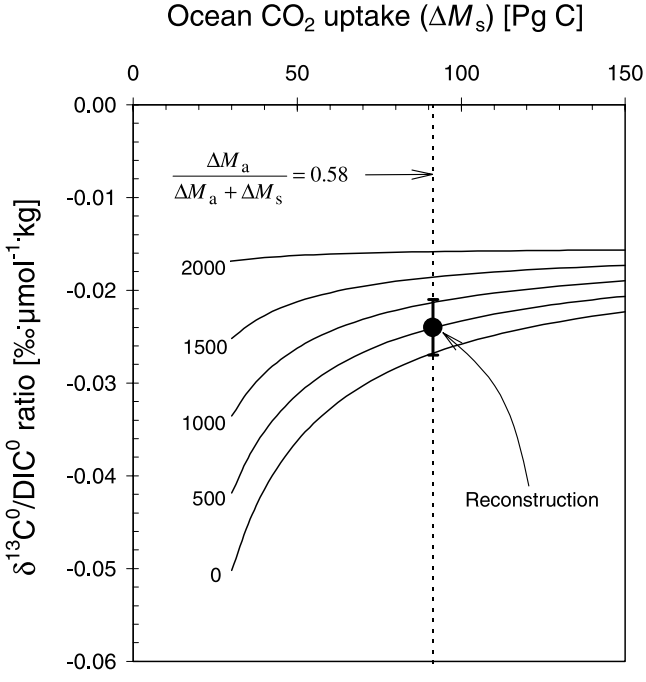

Figure 12. The $\delta^{13}C^0/DIC^0$ perturbation ratio as function of anthropogenic CO_2 uptake in the ocean for different values of the size of the exchangeable biospheric carbon reservoir (values in Pg C).

[58] Following this approach, the $\delta^{13}C^0$-DIC^0 relationship ($\Delta\delta_s/\Delta C_T$ in equation (11)) can be calculated as a function of the total ocean CO_2 uptake (ΔM_s) for different sizes of the exchangeable terrestrial biosphere covering the range of possible scenarios from no exchangeable carbon ($M_b^0 = 0$ Pg C) to fully exchangeable carbon ($M_b^0 = 2000$ Pg C). Using the airborne fraction ($\Delta M_a/(\Delta M_a + \Delta M_s)$) of 0.58 from the work of *Sarmiento et al.* [1992], the 128 Pg C increase of the atmospheric carbon reservoir corresponds to a total ocean CO_2 uptake of 91 Pg C. With this cumulative ocean uptake, the reconstructed $\delta^{13}C^0$-DIC^0 slope of $-0.024 \pm 0.003‰$ $(\mu mol\ kg^{-1})^{-1}$ indicates that less than half of the total carbon stored in the terrestrial biosphere (520 ± 500 Pg C of a total of 2050 Pg C, *Siegenthaler and Sarmiento* [1993]) has been actively exchanging with the atmosphere during period 1960–1993 (Figure 12).

[59] However, the ~12% uncertainty in the $\delta^{13}C^0$-DIC^0 slope (plus the additional uncertainty associated with the parameters in equation (11)) precludes a reliable determination of the size of the exchangeable carbon reservoir using this approach (Figure 12). Also, for reasons outlined above, we expect the North Atlantic $\delta^{13}C^0$-DIC^0 slope to be significantly larger than the ocean's average, and thus this estimate of the mass of the exchanging terrestrial carbon reservoir is likely too small. A precise determination of the mass of the exchanging terrestrial carbon therefore awaits additional estimates of the $\delta^{13}C$-DIC perturbation ratio such that global coverage and higher precision can be achieved.

[60] Another potentially useful application of the $\delta^{13}C^0$-DIC^0 relationship stems from the fact that the air-sea disequilibrium of $\delta^{13}C$ can be estimated with better preci-

sion than the air-sea CO_2 disequilibrium or ΔpCO_2. The average global air-sea disequilibrium of $\delta^{13}C$ of -0.62 ± 0.1‰ [*Gruber and Keeling*, 2001; P. D. Quay et al., Anthropogenic changes of the $^{13}C/^{12}C$ of dissolved inorganic carbon in the ocean as a tracer of CO_2 uptake, submitted to *Global Biogeochem. Cycles*] is generally larger than seasonal and spatial variability of $\delta^{13}C$ in the surface ocean. In contrast, the average ΔpCO_2 of around 8 μatm (inferred from a global net CO_2 uptake of 2 Pg C yr^{-1}) is up to an order of magnitude smaller than seasonal and spatial pCO_2 variability in the surface ocean [*Takahashi et al.*, 1997]. The reconstructed ratio of the oceanic $\delta^{13}C^0$ and DIC^0 perturbations can be used to estimate the mean air-sea ΔpCO_2. For this purpose, it is converted into the ratio of ^{13}C and ^{12}C concentration changes ($\Delta DI^{13}C/\Delta DIC$), which equals the ratio of the net air-sea fluxes of $^{13}CO_2$ and $^{12}CO_2$ (see equations (8) and (7), respectively)

$$\frac{\Delta DI^{13}C}{\Delta DIC} = \frac{F_{13}}{F_{12}} = \frac{\alpha_k k \alpha_{aq-g} K_H \left(R^g_{CO_2} pCO_2^g - \frac{R_{DIC}}{\alpha_{DIC-g}} pCO_2^{sea} \right)}{k K_H \left(pCO_2^g - pCO_2^{sea} \right)} \quad (12)$$

[61] We can estimate the air-sea ΔpCO_2 after solving equation (12) for pCO_2^{sea}, using global area-weighted means of sea surface temperature (18.4°C [*Levitus and Boyer*, 1994]) and salinity (34.75 [*Levitus et al.*, 1994]) to calculate the fractionation factors, the mean 1960–1993 atmospheric CO_2 concentration ($pCO_2^g \cong xCO_2^g$ = 335.3 ppmv), and atmospheric $\delta^{13}C$-CO_2 (−7.3‰), a global gas exchange rate weighted air-sea $\delta^{13}C$ disequilibrium of -0.62 ± 0.10‰ [*Gruber and Keeling*, 2001; *Quay et al.*, submitted] and our $\delta^{13}C^0$-DIC^0 slope of -0.024 ± 0.003‰ (μmol $kg^{-1})^{-1}$. For this set of values we find a global mean air-sea ΔpCO_2 of 5.4 ± 1.1 μatm, which yields a global net uptake of CO_2 on the order of 1.6 ± 0.3 Pg C yr^{-1} when the exchange coefficient kK_H = 0.067 moles CO_2 m^{-2} yr^{-1} μatm^{-1} after the method of *Tans et al.* [1990] is used.

[62] This result for the global mean ΔpCO_2 and the net uptake of anthropogenic CO_2 is not suited to provide a better global estimate of the oceanic uptake of anthropogenic CO_2 as the North Atlantic is not representative of the world ocean. A global mean of the $\delta^{13}C^0$-DIC^0 relationship would likely be less steep [*McNeill et al.*, 2001] and thus yield a higher net oceanic CO_2 uptake in better agreement with the current understanding. Also, the value of -0.62 ± 0.10‰ applied here for the global air-sea $\delta^{13}C$ disequilibrium may not be valid for the whole period of time that is represented in our analysis. A box-diffusion simulation of ocean $^{12}CO_2$ and $^{13}CO_2$ uptake indicates that during the time period over which our $\delta^{13}C^0$-DIC^0 relationship was determined (late 1960s to 1993), the air-sea disequilibrium increased by about −0.3‰ [*Quay et al.*, submitted]. Using an air-sea disequilibrium of −0.47‰, roughly representative of 1980, instead yielded a ΔpCO_2 of 4.1 μatm and an ocean uptake of 1.2 Pg C yr^{-1} by the same approach as above. An improved determination, based on observations of the temporal evolution of the air-sea $\delta^{13}C$ disequilibrium, awaits analysis of planned CLIVAR repeat hydrography cruise data over the coming decade. These cruises will also provide opportunities to reconstruct $\delta^{13}C$ and DIC changes based on multiparameter approaches [*Sabine et al.*, 1999; *Sonnerup et al.*, 2000; *McNeill et al.*, 2001].

[63] Finally, in order to make the estimated ΔpCO_2 compatible with ΔpCO_2 measurements (such as in the form of the compilation of the work of *Takahashi et al.* [1997]), the pre-industrial CO_2 disequilibrium that arises from an imbalance between (inorganic and organic) carbon inputs through rivers and carbon losses through sedimentation has to be taken into account. The complications associated with this approach for determining the global mean ΔpCO_2 are beyond the scope of this paper and will be discussed in more detail as more determinations of the required carbon system parameter become available. We merely demonstrate here that knowledge of the mean oceanic perturbation ratio has the potential to provide relatively precise, model-independent CO_2 uptake estimates.

7. Summary

[64] Using the back-calculation approach of *Sonnerup et al.* [1999b] for $\delta^{13}C$ and extending it to total dissolved inorganic carbon we calculated the temporal change of DIC and $\delta^{13}C$ along five isopycnals in the upper 1000 m of the North Atlantic Ocean. The anthropogenic changes of 1.21 ± 0.07 μmol kg^{-1} yr^{-1} (DIC) and -0.026 ± 0.002‰ yr^{-1} ($\delta^{13}C$) during 1950–1993 are in good agreement with results from previous studies. That they seem to be on the high end of the range of published values can be explained by the fact that apparent CFC ages are biased young for ages > 25 years. Based on estimated end-member characteristics we find no evidence for significant mixing biases on DIC^0 or $\delta^{13}C^0$. The observed $\delta^{13}C^0$-DIC^0 perturbation ratio of -0.024 ± 0.003‰ (μmol $kg^{-1})^{-1}$ in the North Atlantic Ocean is significantly higher than databased on other oceanic regions, and the global mean from model results.

[65] We used a simple 1D model calibrated to CFCs to investigate reasons why the North Atlantic DIC and $\delta^{13}C$ change rates may be larger than the global average. Our model results indicate that in the case of CO_2, surface waters are able to stay close to equilibrium with the anthropogenic perturbation. For DIC, the observed temporal change slightly exceeds the thermodynamically driven equilibrium uptake. This points toward an enhancement of the uptake of anthropogenic CO_2. The oceanic ^{13}C perturbation follows the atmospheric ^{13}C history with a roughly decadal lag due to the long equilibration time-scale of ^{13}C. Our model results suggest that this delay can cause the $\delta^{13}C^0$-DIC^0 slope to exceed that found in the atmospheric time history due to a recent decrease of the atmospheric $\delta^{13}C$ decrease rate.

[66] We were able to reproduce temporal DIC^0 and $\delta^{13}C^0$ trends as well as the $\delta^{13}C^0$-DIC^0 relationship reasonably well using the 1D advection-diffusion. Significant biases due to the influence of zonal transports on tracer fields could be ruled out, and scaling calculations indicated that our isopycnal analysis was not strongly biased by end-member mixing effects. Absolute values of DIC^0 and $\delta^{13}C^0$ were not well reproduced by the model because the real ocean is not in equilibrium with the atmosphere while the model was initiated at equilibrium. The actual air-sea disequilibrium for CO_2 and ^{13}C in the North Atlantic Ocean

is maintained by biological carbon export, CO_2 gas exchange, and circulation processes that are not represented in the model.

[67] Because of the one order of magnitude difference in the two tracers' timescale for equilibration between the surface mixed layer and the atmosphere – 1 year for DIC and 10 years for DI^{13}C – reconstructions of DIC^0 and $\delta^{13}C^0$ provide useful information about processes controlling air-sea CO_2 disequilibrium conditions. The situation found in the North Atlantic, where reconstructed anthropogenic DIC and $\delta^{13}C$ changes can reasonably well be explained by prevailing disequilibrium conditions, may not be representative of the world ocean. In regions where surface water exposure times to the atmosphere are short relative to the equilibration timescale of $\delta^{13}C$ significantly less steep perturbation ratios can be expected.

[68] Precise knowledge of the global ocean's DIC^0-$\delta^{13}C^0$ relationship would not only provide powerful constraints on changes of the oceanic carbon inventory and the ^{13}C Suess effect, but could be used to constrain the size of the exchangeable terrestrial carbon reservoir and most notably to estimate the mean air-sea pCO_2 equilibrium. Our results of these applications using the North Atlantic results only are in general agreement with the current understanding of the perturbed oceanic carbon cycle. The results are indicative of a rather slow overturning in the North Atlantic that can be viewed as a manifestation of the thermohaline circulation. As the perturbation ratio found in the North Atlantic is likely not representative of the world ocean, these results are shown to demonstrate the potential of these approaches, and to encourage further work in determining the global $\delta^{13}C^0$-DIC^0 perturbation ratio and air-sea $\delta^{13}C$ disequilibrium.

Appendix A: Calculation of Preformed Alkalinity

[69] The calculation of preformed DIC (equations (1) and (2)) requires estimation of a sample's preformed alkalinity (A_T^0). Unlike DIC, seawater alkalinity is not affected by the invasion of (anthropogenic) CO_2 from the atmosphere and preformed alkalinity should therefore have remained constant over the time span of the anthropogenic perturbation. Surface seawater alkalinity shows quasi-conservative behavior, and it is common practice [e.g., *Millero et al.*, 1998] to normalize total alkalinity to a constant salinity ($nA_T = A_T35/S$) and use the observed $nA_T - \theta$ relationship (equation (A1), for $10 < \theta < 21°C$) to calculate A_T^0 at a salinity of 35

$$nA_T^0(\pm 2.5) = -0.6(\pm 0.1)\theta + 2318.1(\pm 1.6) \quad \text{(A1)}$$

This practice, however, neglects the fact that the A_T–S relationship is characterized by a significant intercept representing the freshwater end-member (equation (A2)). By implicitly assuming a zero intercept in the normalization procedure spurious variance is added to the salinity normalized alkalinity. In this study, traditionally normalized alkalinity ($(nA_T = A_T35/S)$) deviated by −8 to 4 μmol/kg from the alkalinity normalized using the slope of the A_T–S relationship (equation (A2)) over the observed salinity range ($S = 36.6 - 34.5$).

$$A_T^0(\pm 5.5) = 58.1(\pm 0.6)S + 273(\pm 23) \quad \text{(A2)}$$

[70] Equation (A2) provides a more accurate means of salinity normalization. Over the temperature range 10°–21°C, alkalinity normalized using equation (A2) does not show a temperature dependence (slope = 0.02 ± 0.10). The temperature dependence observed for traditionally normalized alkalinity (equation (A1)) thus appears to be largely fortuitous and due to the spurious variance added by the normalization procedure itself. For temperatures above 21°C even alkalinities normalized using equation (A2) retain some temperature dependence. Thus a multilinear regression of total alkalinity on temperature and salinity (equation (A3), $10 < \theta < 28°C$) provides a more robust means of estimating preformed alkalinity over the whole range of sea surface temperatures. In all present calculations equation (A3) was used instead of equation (A2)

$$A_T^0(\pm 4.1) = -0.79\theta(\pm 0.07) + 60.9S(\pm 0.5) + 189(\pm 19) \quad \text{(A3)}$$

Appendix B: Calculation of DIC and $\delta^{13}C$ Air-Sea Equilibrium

[71] The equilibrium DIC value was calculated from (annual mean) outcrop T and S, preformed alkalinity A_T^0 (equation (A3)), and the pre-industrial CO_2 mole fraction (xCO_2 = 276.9 ppmv in 1765) by applying the thermodynamic relationships of the marine CO_2 system and assuming no pre-industrial pCO_2 air-sea disequilibrium. All CO_2 system calculations were carried out using the software program of *Lewis and Wallace* [1998] and the carbonic acid dissociation constants after the work by *Mehrbach et al.* [1973] (refit by *Dickson and Millero* [1987]). This calculation procedure also yielded values for the Revelle factor, f_R, and the carbonate fraction of DIC, $f_{CO_3^{2-}}$, representing the surface ocean CO_2 system at each isopycnal's outcrop. Both properties are needed in air-sea exchange parameterization for CO_2 and ^{13}C as described below.

[72] For ^{13}C, the equilibrium fractionation between DIC and gaseous CO_2 has to be taken into account, which depends on temperature and carbon speciation within the marine CO_2 system. *Zhang et al.* [1995] measured the equilibrium enrichment ($\varepsilon_{DIC\text{-}g}$) of ^{13}C in seawater DIC and obtained the following empirical function for $T = 5 - 25°C$ and $f_{CO_3^{2-}} = 0.05 - 0.20$

$$\varepsilon_{DIC-g} = -0.107T + 10.53 + 0.014Tf_{CO_3^{2-}} \quad \text{(B1)}$$

The $\delta^{13}C$ of surface seawater DIC in equilibrium with the pre-industrial atmosphere ($\delta^{13}C_g = -6.30‰$ in 1765) can then be calculated using climatological T at each isopycnal's outcrop

$$\delta^{13}C = \varepsilon_{DIC-g} + \delta^{13}C_g \quad \text{(B2)}$$

Appendix C: Bulk Formula for Net Air-Sea Exchange of $^{13}CO_2$

[73] The bulk formula for the net air-sea exchange of $^{13}CO_2$, F_{13}, can be derived from the bulk formula for the net air-sea exchange of $^{12}CO_2$ (equation (7))

$$F_{13} = k^{13}\left(K_H^{13}R_{CO_2}^{g}pCO_2^{g} - K_H R_{CO_2}^{sea}pCO_2^{sea}\right) \quad \text{(C1)}$$

where $R^{g}_{CO_2}$ and $R^{sea}_{CO_2}$ represent the $^{13}C/^{12}C$ ratios of CO_2 in air and seawater (CO_2(aq)), respectively, and $K_H{}^{13}$ is the solubility of $^{13}CO_2$. Equation (C1) illustrates that F_{13} not only depends on the CO_2 gradient but also on the isotopic disequilibrium. The ^{12}C and ^{13}C flux properties are related through the kinetic fractionation factor of CO_2 gas transfer, α_k, and the equilibrium fractionation factor for CO_2 gas dissolution α_{aq-g}

$$\alpha_k = \frac{k_{13}}{k} \tag{C2}$$

$$\alpha_{aq-g} = \frac{K_H^{13}}{K_H} \tag{C3}$$

Using equations (C2) and (C3) and replacing $R^{sea}_{CO_2}$ by $R_{DIC}/\alpha_{DIC-g}\alpha_{ac-g}$, equation (C1) can be rewritten as follows:

$$F_{13} = \alpha_k k \alpha_{aq-g} K_H \left(R^{g}_{CO_2} pCO_2^{g} - \frac{R_{DIC}}{\alpha_{DIC-g}} pCO_2^{sea} \right) \tag{C4}$$

[74] **Acknowledgments.** The $\delta^{13}C$ measurements were made with support of the NOAA/OACES program under grant NA86GP0104. Arne Körtzinger is particularly grateful to Paul Quay for providing the opportunity to work at the University of Washington, and to the Deutsche Forschungsgemeinschaft for funding this research stay. Finally we would like to acknowledge the comments of two anonymous reviewers, which helped to improve the manuscript. This is JISAO contribution number 837.

References

Anderson, L. A., On the hydrogen and oxygen content of marine phytoplankton, *Deep Sea Res.*, *42*, 1675–1680, 1995.

Anderson, L. A., and J. L. Sarmiento, Redfield ratios of remineralization determined by nutrient data analysis, *Global Biogeochem. Cycles*, *8*, 65–80, 1994.

Andres, R. J., G. Marland, T. Boden, and S. Bischof, Carbon dioxide emissions from fossil fuel consumption and cement manufacture, 1751 to 1991, and an estimate of their isotopic composition and latitudinal distribution, in *The Carbon Cycle*, edited by T. M. L. Wigley and D. S. Schimel, pp. 53–62, Cambridge University Press, New York, 2000.

Armi, L., and H. Stommel, Four views of a portion of the North Atlantic subtropical gyre, *J. Phys. Oceanogr.*, *13*, 828–857, 1983.

Bacastow, R. B., C. D. Keeling, T. J. Lueker, M. Wahlen, and W. G. Mook, The $\delta^{13}C$ Suess effect in the world surface oceans and its implications for oceanic uptake of CO_2: Analysis of observations at Bermuda, *Global Biogeochem. Cycles*, *10*, 335–346, 1996.

Bates, N. R., Interannual variability of oceanic CO_2 and biogeochemical properties in the Western North Atlantic subtropical gyre, *Deep Sea Res., Part II*, *48*, 1507–1528, 2001.

Bates, N. R., A. F. Michaels, and A. H. Knap, Seasonal and interannual variability of oceanic carbon dioxide species at the U.S. JGOFS Bermuda Atlantic Time-series Study (BATS) site, *Deep Sea Res., Part II*, *43*, 347–383, 1996.

Böhm, F., M. M. Joachimski, H. Lehnert, G. Morgenroth, W. Kretschmer, J. Vacelet, and W.-Chr. Dullo, *Earth Planet. Sci. Lett.*, *139*, 291–303, 1996.

Bonneau, M.-C., C. Bergnaud-Grazzini, and W. H. Berger, Stable isotope fractionation and differential dissolution in recent planktonic foraminifera from Pacific box cores, *Oceanol. Acta*, *3*, 377–382, 1980.

Brewer, P. G., Direct observation of the oceanic CO_2 increase, *Geophys. Res. Lett.*, *5*, 997–1000, 1978.

Broecker, W. S., and E. Maier-Reimer, The influence of air and sea exchange on the carbon isotope distribution in the sea, *Global Biogeochem. Cycles*, *6*, 315–320, 1992.

Bullister, J. L., and R. F. Weiss, Determination of CCl_3F and CCl_2F_2 in seawater and air, *Deep Sea Res.*, *35*, 839–853, 1988.

Dickson, A. G., and F. J. Millero, A comparison of the equilibrium constants for the dissociation constants of carbonic acid in seawater media, *Deep Sea Res.*, *34*, 1733–1743, 1987.

Doney, S. C., and J. L. Bullister, A chlorofluorocarbon section in the eastern North Atlantic, *Deep Sea Res.*, *39*, 1857–1883, 1992.

Druffel, E. R. M., and L. M. Benavides, Input of excess CO_2 to the surface ocean based on based on C-13/C-12 ratios in a banded Jamaican sclerosponge, *Nature*, *321*, 58–61, 1986.

Fletcher, C. A. J., *Computational Techniques for Fluid Dynamics*, p. 409, Springer, New York, 1988.

Francey, R. J., C. E. Allison, D. M. Etheridge, C. M. Trudinger, I. G. Enting, M. Leuenberger, R. L. Langenfelds, E. Michel, and L. P. Steele, A 1000-year high precision record of $\delta^{13}C$ in atmospheric CO_2, *Tellus Ser. B*, *51*, 170–193, 1999.

Goericke, R., and B. Fry, Variations of marine plankton $\delta^{13}C$ with latitude, temperature, and dissolved CO_2 in the world ocean, *Global Biogeochem. Cycles*, *8*, 85–90, 1994.

Gruber, N., and C. D. Keeling, An improved estimate of the isotopic air-sea disequilibrium of CO_2: Implications for the oceanic uptake of anthropogenic CO_2, *Geophys. Res. Lett.*, *28*, 555–558, 2001.

Gruber, N., J. L. Sarmiento, and T. F. Stocker, An improved method for detecting anthropogenic CO_2 in the oceans, *Global Biogeochem. Cycles*, *8*, 809–837, 1996.

Gruber, N., C. D. Keeling, and T. F. Stocker, Carbon-13 constraints on the seasonal inorganic carbon budget at the BATS site in the northwestern Sargasso Sea, *Deep Sea Res., Part I*, *45*, 673–717, 1998.

Gruber, N., C. D. Keeling, R. B. Bacastow, P. R. Guenther, T. J. Lueker, M. Wahlen, H. A. J. Meijer, W. G. Mook, and T. F. Stocker, Spatiotemporal patterns of carbon-13 in the global surface ocean and the oceanic Suess effect, *Global Biogeochem. Cycles*, *13*, 307–335, 1999.

Heimann, M., and E. Maier-Reimer, On the relations between the oceanic uptake of CO_2 and its carbon isotopes, *Global Biogeochem. Cycles*, *10*, 89–110, 1996.

Jenkins, W. J., Determination of isopycnal diffusivity in the Sargasso Sea, *J. Phys. Oceanogr.*, *21*, 1058–1061, 1991.

Johnson, K. M., K. D. Wills, D. B. Butler, W. K. Johnson, and C. S. Wong, Coulometric total carbon dioxide analysis for marine studies: maximizing the performance of an automated gas extraction system and coulometric detector, *Mar. Chem.*, *44*, 167–187, 1993.

Joos, F., G. K. Plattner, T. F. Stocker, O. Marchal, and A. Schmittner, Global warming and marine carbon cycle feedbacks an future atmospheric CO_2, *Science*, *284*, 464–467, 1999.

Keeling, C. D., and T. P. Whorf, Atmospheric CO_2 records from sites in the SIO air sampling network, in *Trends: A Compendium of Data on Global Change*, Carbon Dioxide Information Analysis Center, Oak Ridge National Laboratory, U.S. Dept. of Energy, Oak Ridge, Tenn., 2000.

Keir, R., G. Rehder, E. Suess, and H. Erlenkeuser, The $\delta^{13}C$ anomaly in the northeastern Atlantic, *Global Biogeochem. Cycles*, *12*, 467–477, 1998.

Klein, B., and M. Tomczak, Identification of diapycnal mixing through optimum multiparameter analysis, 2, Evidence for unidirectional diapycnal mixing in the front between North and South Atlantic Central Water, *J. Geophys. Res.*, *C 99*, 25,175–25,280, 1994.

Körtzinger, A., L. Mintrop, and J. C. Duinker, On the penetration of anthropogenic CO_2 into the North Atlantic Ocean, *J. Geophys. Res.*, *C 103*, 18,681–18,689, 1998.

Körtzinger, A., M. Rhein, and L. Mintrop, Anthropogenic CO_2 and CFCs in the North Atlantic Ocean—A comparison of man-made tracers, *Geophys. Res. Lett.*, *26*, 2065–2068, 1999.

Körtzinger, A., J. I. Hedges, and P. D. Quay, Redfield ratios revisited: Removing the biasing effect of anthropogenic CO_2, *Limnol. Oceanogr.*, *46*, 964–970, 2001a.

Körtzinger, A., W. Koeve, P. Kähler, and L. Mintrop, C:N ratios in the mixed layer during the productive season in the Northeast Atlantic Ocean, *Deep Sea Res., Part I*, *48*, 661–688, 2001b.

Kroopnick, P. M., The distribution of ^{13}C of ΣCO_2 in the world oceans, *Deep Sea Res.*, *32*, 57–84, 1985.

Levitus, S., and T. P. Boyer, *World Ocean Atlas 1994*, vol. 4, Temperature, Atlas NESDIS 4, National Oceanographic Data Center, Silver Spring, Maryland, 1994.

Levitus, S., R. Burgett, and T. P. Boyer, *World Ocean Atlas 1994*, vol. 3: Salinity, Atlas NESDIS 3, National Oceanographic Data Center, Silver Spring, Maryland, 1994.

Lewis, E., and D. W. R. Wallace, Program developed for CO_2 system calculations, Carbon Dioxide Information Analysis Center, *Report ORNL/CDIAC-105*, Oak Ridge National Laboratory, Oak Ridge, Tenn., 1998.

Lynch-Stieglitz, J., T. F. Stocker, W. S. Broecker, and R. G. Fairbanks, The influence of air-sea exchange on the isotopic composition of oceanic carbon: Observations and modeling, *Global Biogeochem. Cycles*, *9*, 653–665, 1995.

Meier-Reimer, E., and K. Hasselmann, Transport and storage of CO_2 in the ocean—an inorganic ocean-circulation carbon cycle model, *Clim. Dyn.*, *2*, 63–90, 1987.

Martin, J. H., G. A. Knauer, D. M. Karl, and W. W. Broenkow, VERTEX: Carbon cycling in the northeast Pacific, *Deep Sea Res.*, *34*, 267–285, 1987.

McGuire, A. D., et al., Carbon balance of the terrestrial biosphere in the twentieth century: Analyses of CO_2, climate and land use effects with four process-based ecosystem models, *Global Biogeochem. Cycles*, *15*, 183–206, 2001.

McNeill, B. I., R. J. Matear, and B. Tilbrook, Does carbon 13 track anthropogenic CO_2 in the Southern Ocean? Global Biogeochem, *Cycles*, *15*, 597–614, 2001.

Mehrbach, C., C. H. Culberson, J. E. Hawley, and R. M. Pytkowicz, Measurement of the apparent dissociation constants of carbonic acid in seawater at atmospheric pressure, *Limnol. Oceanogr.*, *18*, 897–907, 1973.

Millero, F. J., J. Z. Zhang, K. Lee, and D. M. Campbell, Titration alkalinity of seawater, *Mar. Chem.*, *44*, 153–165, 1993.

Millero, F. J., K. Lee, and M. Roche, Distribution of alkalinity in the surface waters of the major oceans, *Mar. Chem.*, *60*, 111–130, 1998.

Minster, J. F., and M. Bouhladid, Redfield ratios along isopycnal surfaces - a complementary study, *Deep Sea Res.*, *34*, 1981–2003, 1987.

Monterey, G., and S. Levitus, *Seasonal Variability of Mixed Layer Depth for the World Ocean*, Atlas NESDIS 14, National Oceanographic Data Center, Silver Spring, Maryland, 1997.

Neftel, A., H. Friedli, E. Moor, H. Lötscher, H. Oeschger, U. Siegenthaler, and B. Stauffer, Historical CO_2 record from the Siple Station ice core, in *Trends: A Compendium of Data on Global Change*, Carbon Dioxide Information Analysis Center, Oak Ridge National Laboratory, U.S. Dept. of Energy, Oak Ridge, Tenn., 1994.

Pilson, M. E. Q., *An Introduction to the Chemistry of the Sea*, p. 431, Prentice-Hall, Upper Saddle River, NJ, 1998.

Quay, P. D., B. Tilbrook, and C. S. Wong, Oceanic uptake of fossil fuel CO_2: Carbon-13 evidence, *Science*, *256*, 74–79, 1992.

Redfield, A. C., On the proportions of organic derivatives in sea water and their relation to the composition of plankton, in *James Johnstone Memorial Volume*, pp. 176–192, Liverpool, 1934.

Redfield, A. C., B. H. Ketchum, and F. A. Richards, The influence of organisms on the composition of sea water, in *The Sea*, vol. 2, edited by M. N. Hill, pp. 26–77, Interscience, New York, 1963.

Sabine, C. L., R. M. Key, K. M. Johnson, F. J. Millero, A. Poisson, J. L. Sarmiento, D. W. R. Wallace, and C. D. Winn, Anthropogenic CO_2 inventory of the Indian Ocean, *Global Biogeochem. Cycles*, *13*, 179–198, 1999.

Sarmiento, J. L., and E. T. Sundquist, Revised budget for the oceanic uptake of anthropogenic CO_2, *Nature*, *356*, 589–593, 1992.

Sarmiento, J. L., J. C. Orr, and U. Siegenthaler, A perturbation simulation of CO_2 uptake in an ocean general circulation model, *J. Geophys. Res.*, *97*, 3621–3645, 1992.

Siegenthaler, U., and J. L. Sarmiento, Atmospheric carbon dioxide and the ocean, *Nature*, *365*, 119–125, 1993.

Sonnerup, R. E., On the relations among CFC derived water mass ages, *Geophys. Res. Lett.*, *28*, 1739–1742, 2001.

Sonnerup, R. E., P. D. Quay, and J. L. Bullister, Thermocline ventilation and oxygen utilization rates in the subtropical North Pacific based on CFC distributions during WOCE, *Deep Sea Res., Part I*, *46*, 777–805, 1999a.

Sonnerup, R. E., P. D. Quay, A. P. McNichol, J. L. Bullister, T. A. Westby, and H. L. Anderson, Reconstructing the oceanic ^{13}C Suess effect, *Global Biogeochem. Cycles*, *13*, 857–872, 1999b.

Sonnerup, R. E., P. D. Quay, and A. P. McNichol, The Indian Ocean ^{13}C Suess effect, *Global Biogeochem. Cycles*, *14*, 857–873, 2000.

Speer, K. G., A note on average cross-isopycnal mixing in the North Atlantic Ocean, *Deep Sea Res., Part I*, *44*, 1981–1990, 1997.

Suess, H. E., Natural radiocarbon and the rate of exchange of carbon dioxide between the atmosphere and the sea, in *Nuclear Processes in Geologic Settings*, edited by National Research Council Committee on Nuclear Science, pp. 52–56, National Academy of Sciences, Washington, D. C., 1953.

Sundquist, E. T., L. N. Plummer, and T. M. L. Wigley, Carbon dioxide in the ocean surface: The homogeneous buffer factor, *Science*, *204*, 1203–1205, 1979.

Takahashi, T., W. S. Broecker, and S. Langer, Redfield ratio based on chemical data from isopycnal surfaces, *J. Geophys. Res.*, *90*, 6907–6924, 1985.

Takahashi, T., T. T. Takahashi, and S. C. Sutherland, An assessment of the role of the North Atlantic as a CO_2 sink, *Phil. Trans. R. Soc. Lond. B*, *348*, 143–152, 1995.

Takahashi, T., R. A. Feely, R. F. Weiss, R. H. Wanninkhof, D. W. Chipman, S. C. Sutherland, and T. T. Takahashi, Global air-sea flux of CO_2: An estimate based on measurements of sea-air pCO_2 difference, *Proc. Natl. Acad. Sci. USA*, *94*, 8292–8299, 1997.

Takahashi, T., et al., Global sea-air CO_2 flux based on climatological surface ocean pCO_2, and seasonal biological and temperature effects, *Deep Sea Res., Part I*, in press, 2002.

Tans, P. P., I. Y. Fung, and T. Takahashi, Observational constraints on the global atmospheric CO_2 budget, *Science*, *247*, 1431–1438, 1990.

Tans, P. P., J. A. Berry, and R. F. Keeling, Oceanic $^{13}C/^{12}C$ uptake observations: A new window on ocean CO_2 uptake, *Global Biogeochem. Cycles*, *7*, 353–368, 1993.

Walker, S. J., R. F. Weiss, and P. K. Salameh, Reconstructed histories of the annual mean atmospheric mole fractions for the halocarbons CFC-11, CFC-12, CFC-113, and carbon tetrachloride, *J. Geophys. Res.*, *105*, 14,285–14,296, 2000.

Wanninkhof, R., Relationship between wind speed and gas exchange over the ocean, *J. Geophys. Res.*, *97*, 7373–7382, 1992.

Wanninkhof, R., S. C. Doney, T.-H. Peng, J. L. Bullister, K. Lee, and R. A. Feely, Comparison of methods to determine the anthropogenic CO_2 invasion into the Atlantic Ocean, *Tellus Ser. B*, *51*, 511–530, 1999.

Warner, M. J., and R. F. Weiss, Solubilities of chlorofluorocarbons 11 and 12 in water and seawater, *Deep Sea Res.*, *32*, 1485–1497, 1985.

Weiss, R. F., The solubility of nitrogen, oxygen and argon in water and seawater, *Deep Sea Res.*, *17*, 721–735, 1970.

Weiss, R. F., Carbon dioxide in water and seawater: the solubility of a non-ideal gas, *Mar. Chem.*, *2*, 203–215, 1974.

Weiss, R. F., and B. A. Price, Nitrous oxide solubility in water and seawater, *Mar. Chem.*, *8*, 347–359, 1980.

Winn, C. D., Y.-H. Li, F. T. Mackenzie, and D. M. Karl, Rising surface ocean dissolved inorganic carbon at the Hawaii Ocean Time-series site, *Mar. Chem.*, *60*, 33–47, 1998.

Zhang, J., P. D. Quay, and D. O. Wilbur, Carbon isotope fractionation during gas-water exchange and dissolution of CO_2, *Geochim. Cosmochim. Acta*, *59*, 107–114, 1995.

A. Körtzinger, and P. D. Quay, School of Oceanography, University of Washington, Seattle, Washington, USA. (akoertzinger@ifm.uni-kiel.de)

R. E. Sonnerup, Joint Institute for Study of the Atmosphere and Ocean, University of Washington, Seattle, Washington, USA. (rolf.sonnerup@noaa.gov)